

INFORMATION TO USERS

This manuscript has been reproduced from the microfilm master. UMI films the text directly from the original or copy submitted. Thus, some thesis and dissertation copies are in typewriter face, while others may be from any type of computer printer.

The quality of this reproduction is dependent upon the quality of the copy submitted. Broken or indistinct print, colored or poor quality illustrations and photographs, print bleedthrough, substandard margins, and improper alignment can adversely affect reproduction.

In the unlikely event that the author did not send UMI a complete manuscript and there are missing pages, these will be noted. Also, if unauthorized copyright material had to be removed, a note will indicate the deletion.

Oversize materials (e.g., maps, drawings, charts) are reproduced by sectioning the original, beginning at the upper left-hand corner and continuing from left to right in equal sections with small overlaps.

Photographs included in the original manuscript have been reproduced xerographically in this copy. Higher quality 6" x 9" black and white photographic prints are available for any photographs or illustrations appearing in this copy for an additional charge. Contact UMI directly to order.

**Bell & Howell Information and Learning
300 North Zeeb Road, Ann Arbor, MI 48106-1346 USA
800-521-0600**

UMI[®]

NOTE TO USERS

This reproduction is the best copy available.

UMI

University of Alberta

**Mutational Analysis of the Homeobox Transcription Factor
PITX2**

By

Stephen Kulak



A thesis submitted to the Faculty of Graduate Studies and Research in
partial fulfillment of the requirements for the degree of Master of Science

in

Medical Sciences - Ophthalmology

Edmonton, Alberta

Fall, 1999



National Library
of Canada

Acquisitions and
Bibliographic Services

395 Wellington Street
Ottawa ON K1A 0N4
Canada

Bibliothèque nationale
du Canada

Acquisitions et
services bibliographiques

395, rue Wellington
Ottawa ON K1A 0N4
Canada

Your file *Votre référence*

Our file *Notre référence*

The author has granted a non-exclusive licence allowing the National Library of Canada to reproduce, loan, distribute or sell copies of this thesis in microform, paper or electronic formats.

The author retains ownership of the copyright in this thesis. Neither the thesis nor substantial extracts from it may be printed or otherwise reproduced without the author's permission.

L'auteur a accordé une licence non exclusive permettant à la Bibliothèque nationale du Canada de reproduire, prêter, distribuer ou vendre des copies de cette thèse sous la forme de microfiche/film, de reproduction sur papier ou sur format électronique.

L'auteur conserve la propriété du droit d'auteur qui protège cette thèse. Ni la thèse ni des extraits substantiels de celle-ci ne doivent être imprimés ou autrement reproduits sans son autorisation.

0-612-47053-9

University of Alberta
Library Release Form

Name of Authour: Stephen Kulak

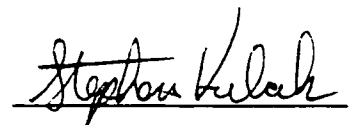
Title of Thesis: Mutational Analysis of the Homeobox Transcription Factor PITX2

Degree: Master of Science

Year Degree Granted: 1999

Permission is hereby granted to the University of Alberta to reproduce single copies of this thesis and to lend or sell such copies for private, scholarly, or scientific research purposes only.

The authour reserves all other publication and other rights in association with the copyright in the thesis, and except as hereinbefore provided, neither the thesis nor any substantial portion thereof may be printed or otherwise reproduced in any material form whatsoever without the authour's prior written permission.



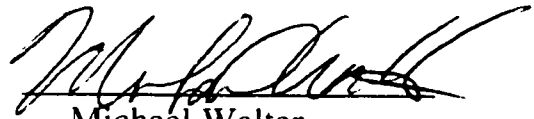
Aug 31/99

#104, 10514-85 Ave.
Edmonton, AB, Canada
T6E 2K4

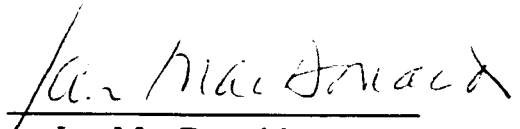
University of Alberta

Faculty of Graduate Studies and Research

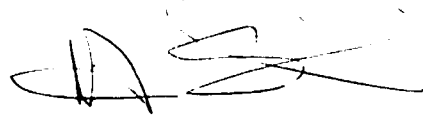
The undersigned certify that they have read, and recommend to the Faculty of Graduate Studies and Research for acceptance, a thesis entitled “ Mutational Analysis of the Homeobox Transcription Factor PITX2”, submitted by Stephen Kulak in partial fulfillment of the requirements for the degree of Master of Medical Sciences in Ophthalmology.



Michael Walter
Associate Professor



Ian MacDonald
Professor



Martin Somerville
Assistant Professor



Moira Glerum
Assistant Professor

Abstract

Axenveld-Rieger syndrome (ARS) is an autosomal dominant disorder which affects the anterior segment of the eye as well as non-ocular structures. ARS patients can present with iris hypoplasia, a prominent Schwalbe line, adhesions between the iris stroma and the irido-corneal angle and increased intra-ocular pressure. ARS also presents with non-ocular features including maxillary hypoplasia, micro and anodontia, redundant peri-umbilical skin, and hypospadias in males. While ARS is genetically heterogeneous, linkage analysis has indicated that a major ARS locus is located at chromosome 4q25. PITX2, also known as RIEG1, the gene responsible for the 4q25 ARS phenotype, has recently been cloned. PITX2 encodes a novel member of the bicoid class of homeobox proteins known to be active as transcription factors. Mutational analysis has previously detected several mutations in PITX2 gene in ARS individuals. The focus of my research is to determine the mutations present in a number of individuals presenting with ARS and to determine any possible genotype/phenotype correlations that may be present. Future work will be directed towards both an understanding of the genetic causes of cases of Axenveld-Rieger syndrome not caused by mutations in the PITX2 gene and analysis of protein/protein interactions of PITX2 with other developmentally important proteins. Characterization of the ARS gene will help elucidate key functional regions of PITX2 and improve our understanding of human developmental biology.

Acknowledgements

It would not have been possible to have completed this work without the assistance of many people. Obviously a great many thanks go to Dr. Michael Walter. His support and guidance made the decision to take on this project one of the best choices I have ever made. Many thanks also to the other members of my committee: Drs. Ian Macdonald and Martin Somerville. Your help and assistance rounded out an excellent grad committee. Thank-you.

To all the people in the Ocular Genetics lab: Farideh, Kerry, Heather, Alan, James, Doug, Dean, Kathy, Donna and Sherry and all the summer students, past and present: you all helped to make the times in the lab into times I will miss. A special thanks to Farideh and Kerry for all you do.

To my parents Nancy and Cliff and to my step parents Susan and Barry: The free meals and laundry were all greatly appreciated. Mountain biking with my brothers and all those e-mail jokes my sister kept sending were also great diversions. Thanks to Bev for the care packages and to Bryce, Jeff and Kara for being such great nephews and niece.

To my friends: Neil and Anna, Bryan and Robyn, Pat and Norma, Lyndon and Lynda, Mark J., Mark F., Jeff, Van and Denise, Kenny, Rick, Dave and Ange, Ted, Will, Tyler, Rod, Terrence, Stuart, Kate, Roman, Leslie, MJ and John, Nick, Barb, Lisa and Jonathon and everyone else: Thanks for everything and here's to future memories...

Table of Contents

	Page
Introduction	
Embryology of the Human Eye.....	1
Development of the Primary Optic Vesicle.....	1
Development of the Optic Vesicle and Mesoderm.....	4
Development of the Anterior Segment of the Eye.....	14
Glaucoma.....	33
History of Axenfeld-Rieger and Iridogoniodysgenesis Syndromes.....	39
Transcription Factors and Eye Development.....	44
Materials.....	52
Methods	
Patients.....	55
Genomic DNA.....	58
PCR Amplification.....	58
PCR Product Purification.....	60
Sequencing.....	60
SSCP Analysis.....	60
Marker Analysis.....	62
Linkage Analysis.....	69
Southern Blots.....	69
Probes for Southern Blots.....	69
Hybridization of Probes to Southern Blots.....	70

Results

SSCP.....	71
Sequencing of the PITX2 Gene	
ADA Family.....	71
RID Family.....	77
Southern Blot Analysis.....	80
Marker Analysis	
Family A.....	83
Family B.....	85
Family C.....	87
PAX6 Mutation in the VA Family.....	89

Discussion

PITX2 missense mutation in a family with IGDS.....	90
PITX2 frameshift mutation in a family with classical ARS.....	94
Genotype/phenotype correlation's in PITX2 mutations.....	97
Frequency of ARS cases caused by PITX2 mutations.....	98
Genes other than PITX2 causing ARS.....	99
Marker Summary.....	101
Vertebrate Development.....	102
PITX2 involvement in Vertebrate Body Plan Development.....	102
PITX2 and interactions with target DNA sites and other proteins.....	103
Haploinsufficiency as a cause of Axenfeld-Rieger Syndrome.....	105
Mechanism of the ARS disorder.....	107

Conclusions.....	110
-------------------------	------------

References.....	111
------------------------	------------

List of Tables

	Title of Table	
		Page
Table 1	Characteristic ocular and non-ocular phenotypes of Axenfeld-Rieger Anomaly and Syndrome (ARA/ARS) and Iridogoniodysgenesis Anomaly and Syndrome (IGDA/IGDS).....	40
Table 2	Phenotypic Characteristics of Patients in PITX2 Mutational Analysis.....	56
Table 3	PCR Primers used to amplify sections of the PITX2 gene.....	61
Table 4	Linkage Results for Family A.....	84
Table 5	Linkage Results for Family B.....	86
Table 6	Linkage Results for Family C.....	88

List of Figures

	Title of Figure	Page
Figure 1	22 day old Human embryo.....	2
Figure 2	Development of the primary optic vesicle.....	5
Figure 3	Early stages of invagination of the primary optic vesicle.....	7
Figure 4	Formation of the optic cup.....	10
Figure 5	Optic cup and lens vesicle in five week old embryo.....	12
Figure 6	Migration of neural crest cells into anterior segment of the eye.....	15
Figure 7	Rudimentary structures of the anterior segment of the eye.....	17
Figure 8	Detail of the differentiating tissues of the anterior segment of the eye.....	20
Figure 9	Relationship between Schlemms Canal and the trabecular meshwork.....	23
Figure 10	Detail of the anterior chamber, marginal sinus and forming iris.....	25
Figure 11	Detail of the anterior angle of the eye indicating tissues affected in ARS/IGDS and ARA/IGDA.....	28
Figure 12	Scanning electron micrograph of anterior segment of 7 month old embryo.....	31
Figure 13	Mature anterior segment of the human eye.....	34
Figure 14	Open angle versus closed angle glaucoma.....	37
Figure 15	Eye and teeth malformations common to ARS/ARA and IGDS/IGDA.....	42
Figure 16	PITX2 gene structure.....	45
Figure 17	Expression profile of the PITX2 gene in the embryonic mouse.....	47
Figure 18	Pedigree of Family A.....	63
Figure 19	Pedigree of Family B.....	65
Figure 20	Pedigree of Family C.....	67
Figure 21	DNA sequence indicating G to A missense mutation in the ADA family.....	73

Figure 22	SSCP analysis of ADA family.....	75
Figure 23	DNA sequence indicating frameshift mutation in the RID family.....	78
Figure 24	Genomic Southern blots probed with PITX2 and FKHL7.....	81
Figure 25	Amino acid sequence comparison of several bicoid class transcription factors.....	91
Figure 26	Location of the two mutations in the PITX2 gene detected in the patient cohort.....	95

Abbreviations

AC= Anterior Chamber
ARA= Axenfeld-Reiger Anomaly
ARS= Axenfeld-Rieger Syndrome
bp= base pairs of DNA
BSA= bovine serum albumin
cM= centimorgans
CP= Ciliary Process
DNA= deoxyribonucleic acid
dNTP= deoxyribonucleotide tri-phosphates
EDTA= Ethylene-diaminetetra-acetic acid disodium salt
g= grams
GTB= Glycerol tolerant buffer
IGDA= Iridgoniodysgenesis Anomaly
IGDS= Iridgoniodysgenesis Syndrome
IOP= Intraocular Pressure
IR= Iris
LOD= Logarithm of odds
MgCl= magnesium chloride
mls= millilitres
MS= marginal sinus
NaCl= sodium chloride
PAX= paired box containing
PCR= polymerase chain reaction
Pitx2= pituitary transcription factor 2
SC= Schlemm's Canal
SSC= sodium chloride and sodium citrate solution
SSCP= single strand conformation polymorphism
TBE= Tris/EDTA/Borate buffer
TM= Trabecular Meshwork
TRIS= Tris(hydroxymethyl)aminomethane
 μ g= microgram
 μ L= microlitre

Introduction

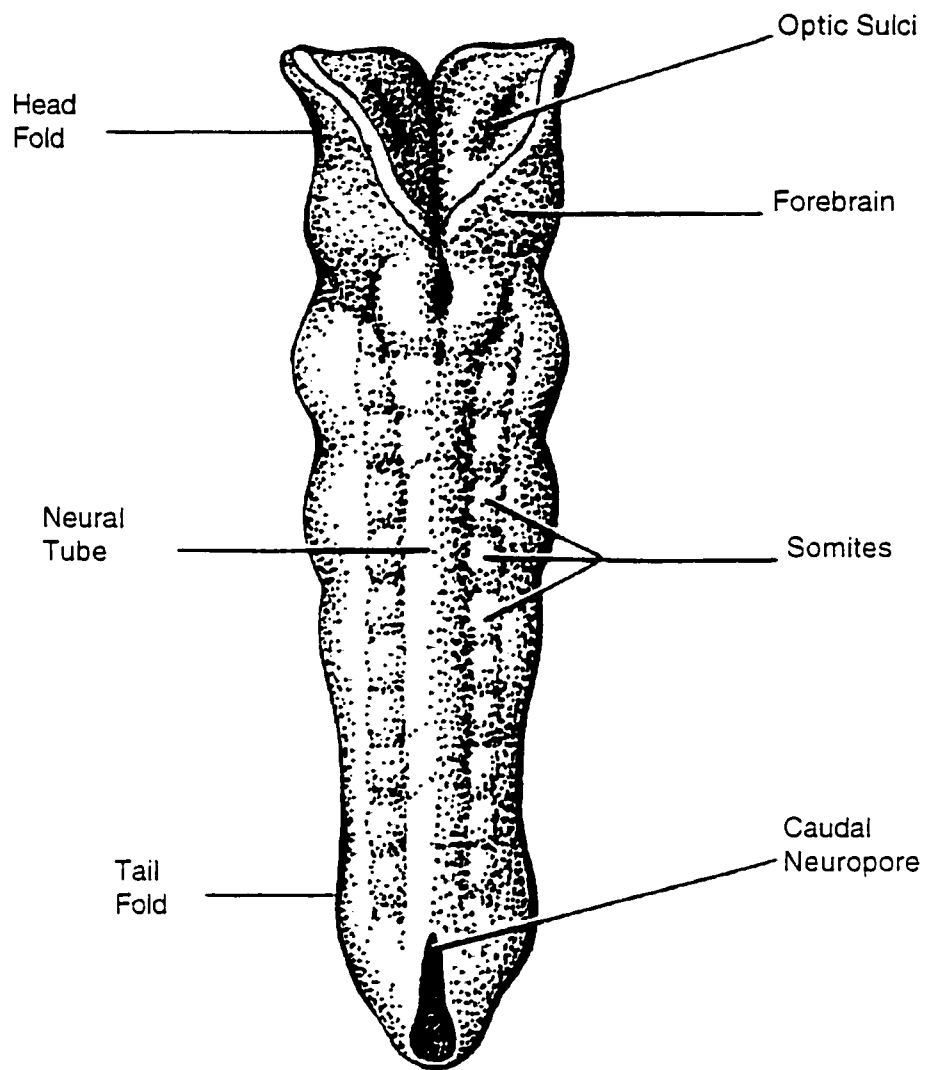
The human eye provides an excellent model tissue to study genetic disease. Twenty-seven percent of all known genetic diseases have some affect on the structure or function of the eye (1). Ocular phenotypic changes are easily observed since the eye is exposed on the surface of the body and even subtle changes in eye structure or function are readily detectable. In addition, genetic diseases affecting the eye are frequently compatible with life such that family studies are often possible. With families available for study, positional cloning strategies can be readily utilized to isolate new genes involved in human disease.

Embryology of the Human Eye

Development of the Primary Optic Vesicle

The rudimentary beginnings of the human eye first appear at approximately 22 days of gestation (1, 2). At this point the three cellular layers of the human embryo (ectoderm, mesoderm, and endoderm) have developed along with the head and tail folds, and the neural groove (Figure 1). As the embryo grows the neural groove begins to close over in the middle of the embryo to start forming the neural tube (Figure 1). Before closure of the neural groove at the cephalic end of the embryo, two optic sulci form on either side of the groove, which are the beginnings of the primary optic vesicles (1, 2). Since the optic vesicles are derived from the same tissue that also goes on to form the brain and spinal cord, the eyes are, from an embryological perspective, outgrowths of the central nervous system. The optic depressions begin to evaginate laterally from the anterior end of the developing embryo. At about the fourth week of growth the neural groove has closed over completely becoming the neural tube (1, 2). This now closes

Figure 1. Diagram illustrating a human embryo (approximately 22 days old). Note the beginnings of the primary optic vesicles referred to as the optic placodes or sulci
(Adapted from (1)).



the optic vesicles off from the exterior environment of the embryo such that the optic vesicles are continuous with the lumen of the developing forebrain (Figure 2). When observed from the outside of the embryo, the optic depressions of the neural groove appear as optic protrusions and are now referred to as the primary optic vesicles. These vesicles are still connected to the lumen of the neural tube by two constrictions referred to as the optic stalks.

Development of the Optic Vesicle and Mesoderm

When the embryo is approximately four weeks old all the principal tissues needed for the eye to form are in place (1, 2). The surface ectoderm will go on to form the lens, corneal epithelium, lacrimal gland and conjunctiva (1, 2). The neural ectoderm gives rise to the retinal pigment epithelium, epithelium of the ciliary processes, the sphincter and dilator muscles of the pupil, the optic nerve, and the pigmented posterior layer of the iris (1, 2). The secondary mesoderm goes on to form the sclera, optic nerve sheath, internal (eg. ciliary muscle) and extraocular muscles, connective tissue, bones of the orbit, the vasculature of the eye (including the Hyaloid artery) and the stroma of the iris (1, 2).

A key feature at this four week stage is the contact that occurs between the neural ectoderm of the primary optic vesicle and the surface ectoderm. This contact occurs at the very apex of the primary optic vesicle and is the area where the lens will form in the surface ectoderm (Figure 3). This area of contact is also where the primary optic vesicle will invaginate to begin forming the optic cup and the future neural retinal layer of the eye (1, 2). In all other areas of the developing embryo a layer of mesoderm is present between the neural ectoderm and the surface ectoderm (1, 2).

The area of the primary optic vesicle in contact with the surface ectoderm begins to flatten slightly while the cells at the contact point become several layers thick. These changes mark the beginning of the invagination of the primary optic vesicle (1, 2). The

Figure 2. Development of the primary optic vesicle. A refers to the surface ectoderm. B refers to the neural ectoderm. For clarity the mesodermal layer between the two ectodermal layers is not indicated (Adapted from (2)).

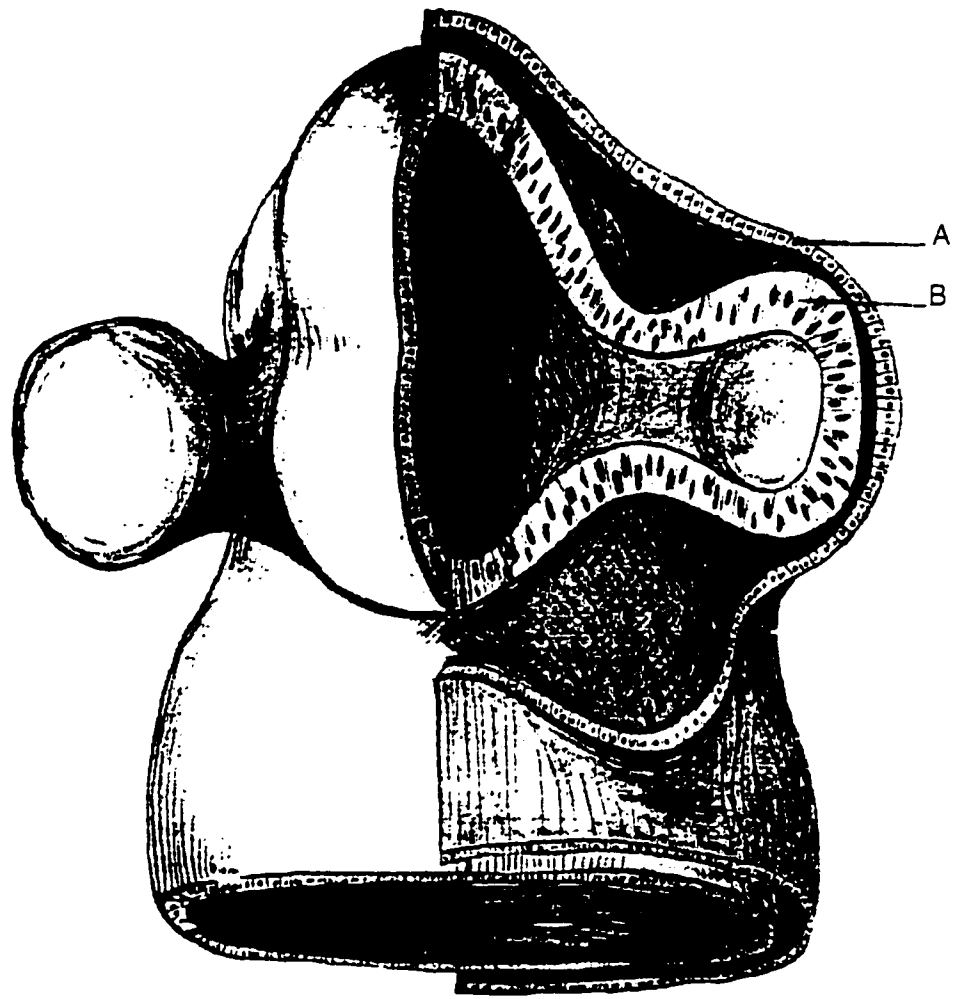
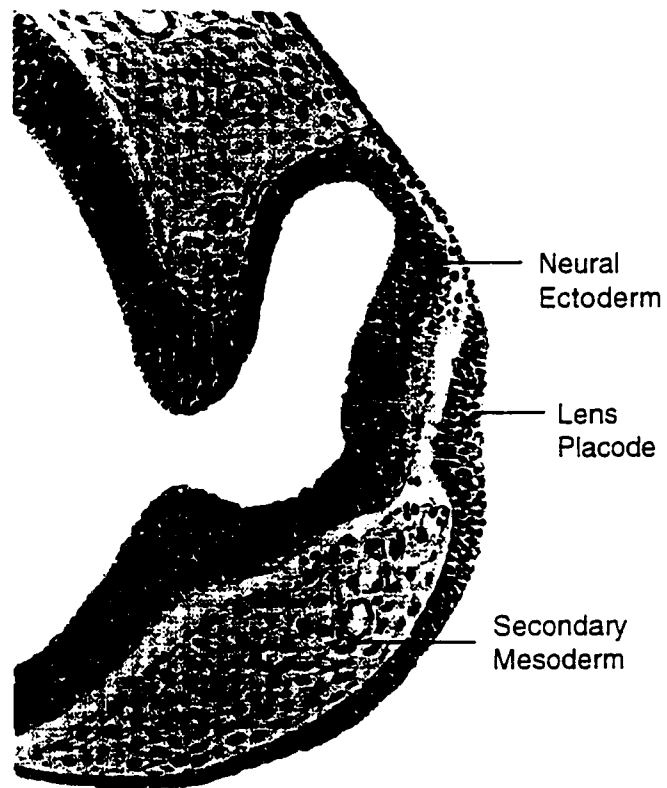


Figure 3. Early stages of invagination of the primary optic vesicle and formation of the lens placode. The lens placode will invaginate to form the lens vesicle. The lens placode also defines the area where the anterior segment and cornea will form
(Adapted from (1)).



primary optic vesicle invaginates as if it were a balloon with force being applied from one direction. The outer layer of the primary optic vesicle will be pushed inwards toward the opposite side until contact is made between the inner layers of the invaginating optic vesicle. The layer of cells which invaginate will form the neural retinal layer while the cells which have remained stationary will form the retinal pigment layer (1, 2) (Figure 4). At the same time the primary optic vesicle is invaginating, a fold is occurring in the posterior aspect of the primary optic vesicle and the optic stalk. This fold is referred to as the embryonic fissure and will form the channel through which the optic nerve will grow. At this time (about five weeks) the embryonic fissure is filled with cells of mesodermal origin. This mesodermal tissue will eventually grow inside the developing optic cup and form a layer between the developing lens and the developing retina (1, 2). Until this point the ectoderm forming the lens and the ectoderm forming the corneal epithelium were in direct contact with each other. The mesodermal cells that enter the forming optic cup will go on to be an integral part of the development of the vitreous, the optic nerve and the vasculature of the eye (1, 2). Invagination of the primary optic vesicle is simultaneous with, and is thought to be responsible for, the thickening and invagination of the cells, which will form the lens. The beginning of the lens placode appears as a thickening of the cells of the surface ectoderm which had been in direct contact with the neural ectoderm (1, 2). As the primary optic cup invaginates, the lens placode also invaginates leading to the formation of a lens pit. As the lens pit deepens it will eventually pinch off and form the lens vesicle. Mesodermal cells will then quickly grow in between the surface ectoderm and the newly formed lens. The surface ectoderm previously in contact with the primitive lens will go on to form the corneal epithelium. The forward edges of the optic cup at five weeks are positioned near the equator of the developing lens. The cells in this portion of the optic cup are still undifferentiated (1, 2) (Figure 5). Separation of the lens from the surface ectoderm occurs when the embryo is approximately five weeks old (1, 2).

Figure 4. Continued invagination of the primary optic vesicle to form the optic cup. Rudimentary double layered retina, lens vesicle, and embryonic fissure all forming (Adapted from (2)).

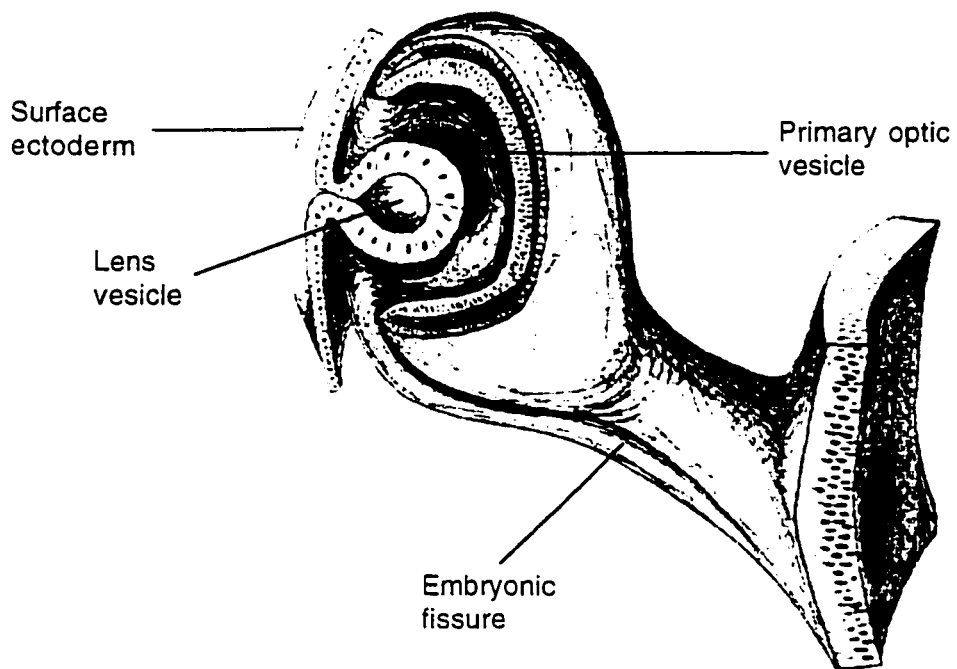


Figure 5. Optic cup and lens vesicle in four to five week old embryo. Anterior edges of optic cup positioned near lens vesicle. Lens vesicle formed and completely covered by surface ectoderm (Adapted from (2)).



Rim of
Optic cup

Lens
vesicle

The eye has now developed what can be viewed as posterior and anterior poles. Since the focus of this study is to deal with the anterior segment disorder, Axenfeld-Rieger syndrome, the embryology and development of the posterior section of the eye will not be considered from this point onwards. Any of the references given for this section can provide the reader with excellent information regarding the development of the posterior of the eye.

Development of the Anterior Segment of the Eye

The anterior segment of the human eye begins to form when the embryo is about 18-20 mm in length which is near the 6th and 7th weeks of gestation (1, 2). During the 6th week of development most activity in the developing eye is confined to the posterior pole, but as the 7th week of development the anterior segment begins to become a recognizable area in the eye (1, 2).

Earlier in development, cells of neural crest origin migrated towards the eye and developed into what is known as periocular mesenchyme or secondary mesenchyme. These mesenchymal cells surround the optic vesicle and optic cup as development proceeds. Around the sixth and seventh week of embryogenesis, the periocular mesenchyme migrates forward towards the anterior pole of the eye in three distinct waves (1, 2) (Figure 6). The first group of cells migrates between the surface ectoderm and the lens. These cells will form the endothelium of the cornea and trabecular meshwork. The second set of neural crest derived cells will go on to form the keratocytes which are the cells which form the stroma of the cornea. The third wave of cells goes on to develop into the anterior stroma of the iris (1, 2).

After the migration of these mesenchymal cells, the specific structures which they form begin to differentiate (1, 2). The rudiments of Descemet's membrane begin to arise from the corneal endothelium cells by week eight (Figure 7). The edge of Descemet's

Figure 6. Migration of neural crest cells into the anterior segment of the developing eye. Wave 1 forms the corneal endothelium. Wave 2 forms the corneal stroma. Wave 3 forms the iris stroma (Adapted from (1)).

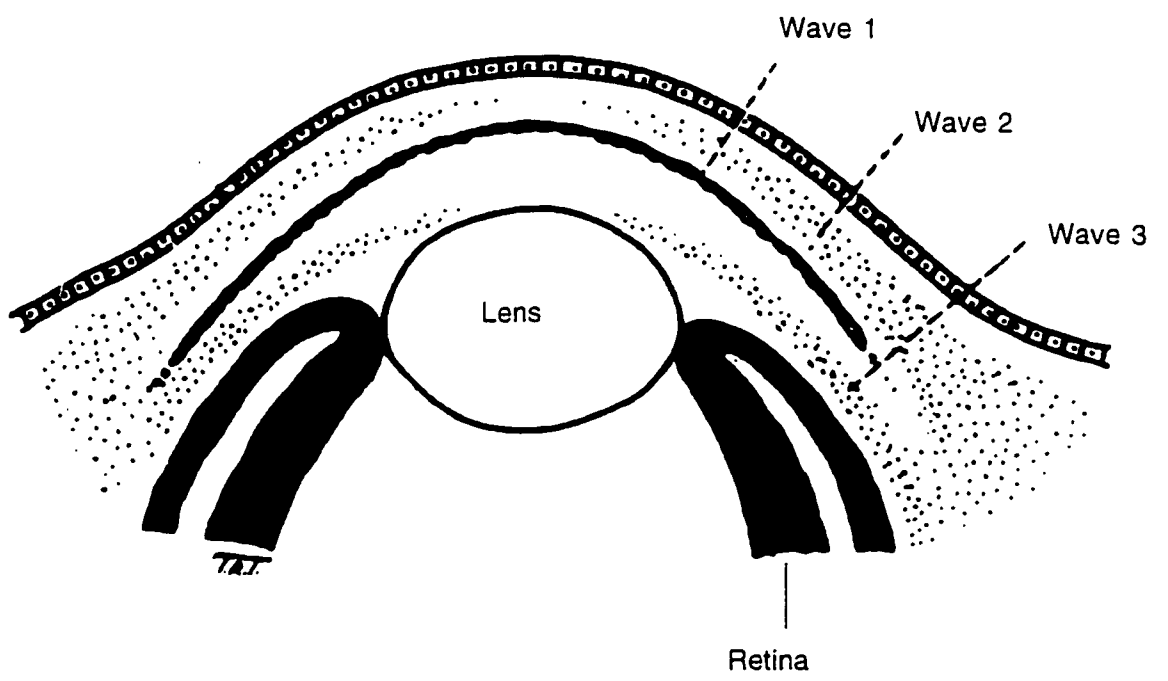
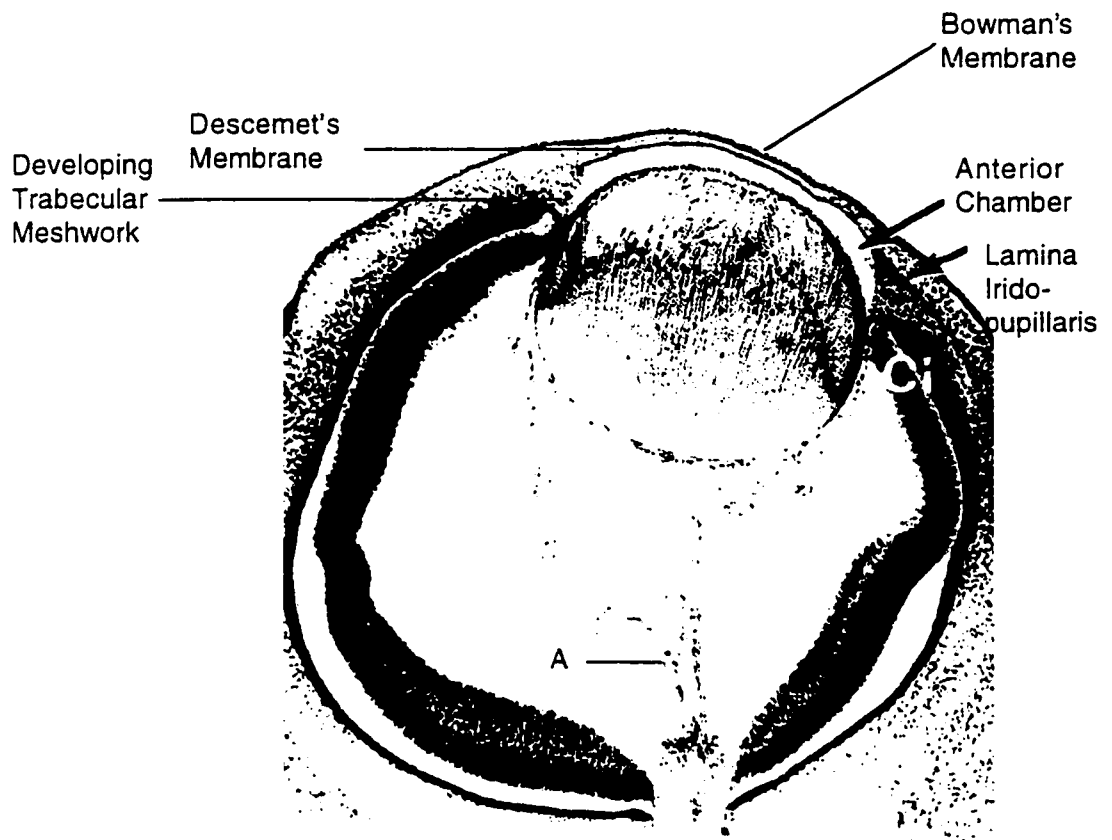


Figure 7. Structure of the rudimentary anterior chamber of the eye. Descemet's and Bowman's membrane are forming. The Anterior segment appears as a thin slit in the front of the eye. "Ci" refers to the beginnings of the ciliary body. "A" refers to the hyaloid artery. The trabecular meshwork will eventually be positioned at the edge of the anterior segment (Adapted (1)).



membrane will define the border with the future trabecular meshwork (Figure 7). As development reaches month 3 (12 weeks) the anterior rim of the optic cup now comes into contact with the lens as the neuroectoderm of the optic cup grows forward towards the anterior edge of the lens. Folds develop in the cells of both the inner and outer layers of the neuroectoderm, a short distance back from the growing edge. These folds will go on to form the ciliary body and ciliary processes (1, 2) (Figure 8). The cells between the ciliary folds and the growing edge of the neuroectoderm go on to develop into the iris epithelium and the pupillary sphincter muscle cells (1, 2) (Figure 13). Corneal development is also proceeding at this time with generalized rapid growth, continued formation of Descemet's membrane, and formation of the limbus (the area of contact between the cornea and sclera). The anterior segment takes on a slit-like appearance at about seven weeks growth. Corneal epithelium cells cover the anterior face of the developing chamber and primitive trabecular meshwork cells and iris stromal cells lining the posterior face (1). During the fourth month of development, the anterior chamber continues to form its distinct structures. The anterior edge of the optic cup continues its forward growth around the lens while the sphincter muscle cells and the iris epithelium continue to develop from the cells of the rapidly growing leading edge of the optic cup. Changes in vascularization play a significant role in eye development at this time.

Formation of the major arterial circle of the iris occurs when some of its branches grow through the mesenchyme of the iris epithelium to form the pupillary membrane. The choriocapillaris grows anteriorly over the developing ciliary body and iris epithelium. Some of the vessels of the choriocapillaris penetrate into the ciliary folds present in the neuroectoderm and transform them into ciliary processes.

During the fourth month, the cornea also continues to differentiate and mature. The corneal stroma becomes thicker while the corneal epithelium remains essentially unchanged. Bowman's membrane can be observed at this time and Descemet's membrane

Figure 8. Illustration showing the beginning of the ciliary process (Cp). The anterior chamber angle (AC), marginal sinus (ms), lens and Iris (Ir), major arterial circle of the iris (cim), are also indicated. Curved arrow indicates the ciliary muscle and straight arrows indicate the vitreous base. (Adapted from (1)).



thickens. The line of demarcation between the cornea and the sclera also becomes easier to observe (Figure 7).

The development of the angle of the anterior chamber and the growth of the ciliary body occur simultaneously at this time (about 4 months). The internal and external cell layers of the ciliary body have differentiated by this stage of growth and it is thought that different rates of growth between these two layers cause the formation of the angle of the anterior chamber (1). At the start of the fourth month of gestation, the ciliary processes are located anterior to the angle of the anterior chamber, and the anterior rim of the optic cup is posterior to the future trabecular meshwork (1, 2). As the leading edge of the optic cup continues to grow forward, the future angle of the anterior chamber is displaced posteriorly. The cells of the future trabecular meshwork have a distinct ultrastructure that distinguishes them from the nearby cells of the cornea (1, 2). The trabecular meshwork will develop intercellular gaps which will form the spaces where vitreous fluid is drained from the eye. It is also believed that Schlemm's canal appears during the fourth month as a bundle of blood vessels anterior to the developing trabecular meshwork. Schlemm's canal is the major drainage route by which aqueous humour is transported to the lymphatic circulatory system (1) (Figure 9).

The anterior segment continues to develop during the fifth month of growth. The anterior neuroectoderm continues to grow, resulting in the development of ciliary channels in the ciliary epithelium. Development of the pupillary sphincter muscle cells continues. The cells of the pupillary sphincter muscle arise from the anterior cells of the marginal sinus. The marginal sinus is the last remaining space of the lumen of the primary optic vesicle (1, 2) (Figure 10). Pigmentation of the posterior iris epithelium begins during the fifth month (1, 2). Vascularization continues to play a key role in the formation of many eye structures. Of particular interest is the major arterial circle of

Figure 9. Figure showing the location of Schlemm's canal and it's relation to the trabecular meshwork (Adapted from (3)).

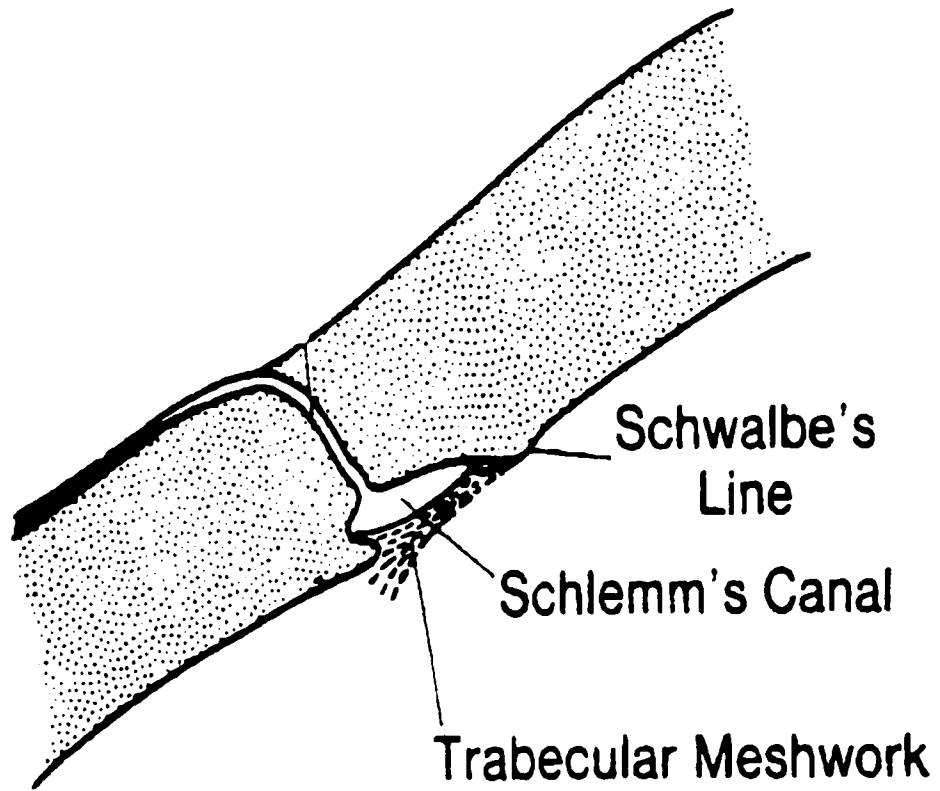
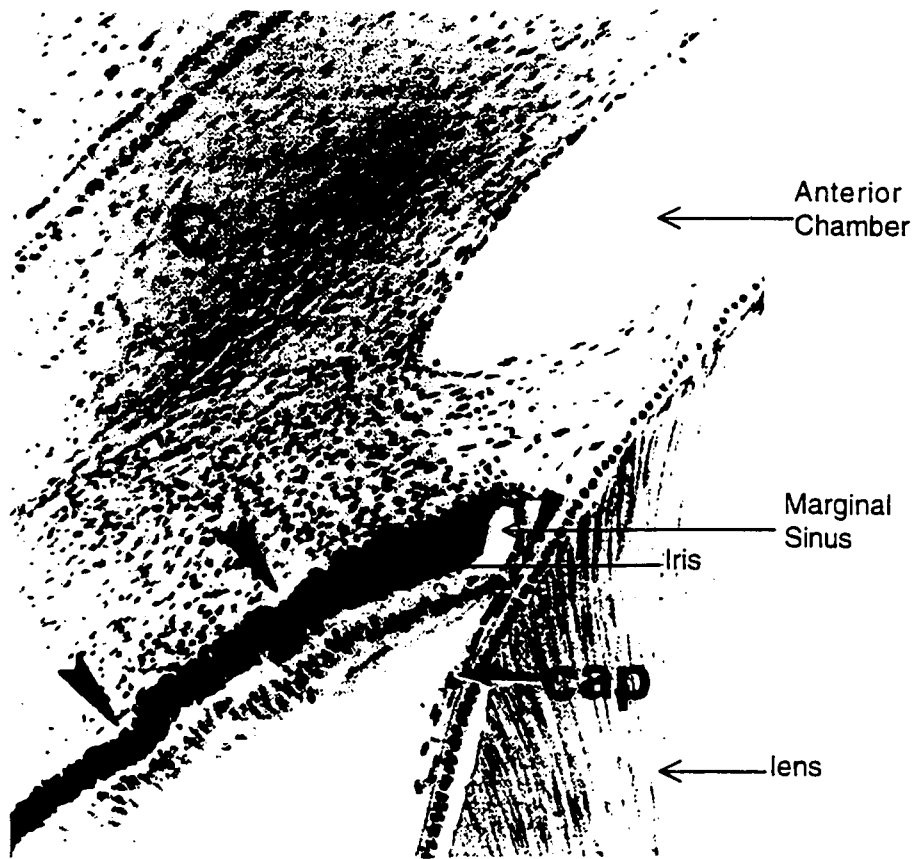


Figure 10. Diagram indicating position of the marginal sinus in the anterior chamber. Also indicated are the forming lens, iris and cornea (C), cap refers to the lateral tunica vasculosa lentis. The arrows indicate the beginnings of the ciliary processes (Adapted from (1)).



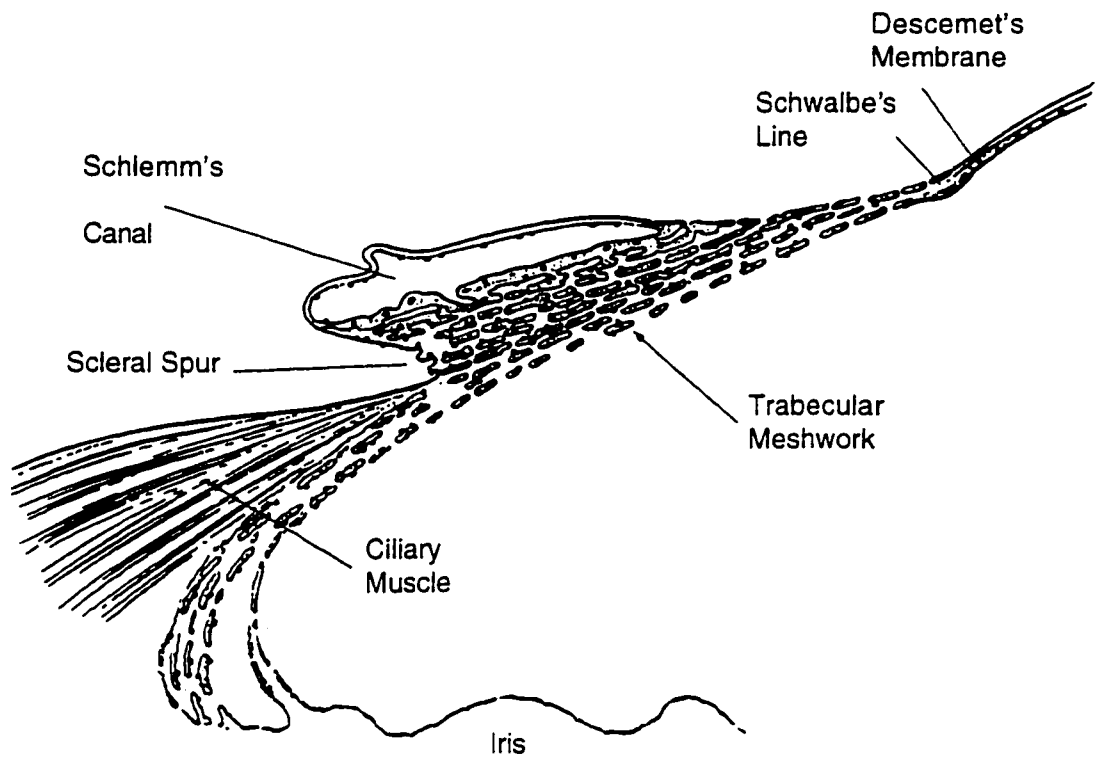
the iris which produces vessels penetrating the ciliary body and into the developing stroma of the iris. Further growth of the iris vessels also contributes to the growth of the pupillary membrane.

The angle of the anterior chamber continues to develop during the fifth month. The trabecular meshwork develops a greater number of intercellular gaps and spaces while the apex of the angle continues to move posteriorly to the ciliary body and processes. The apex of the angle is now located at the future site of Schwalbe's line (1, 2) (Figure 9). Schwalbe's line is the band of tissue which defines the junction of the corneal endothelium with the trabecular meshwork. A common diagnostic criteria of ARS is the anterior displacement of the Schwalbe line (3).

The anterior segment does not undergo any significant changes during the month of development. The dilator pupillae muscle begins to form from anterior neuroectoderm and the sphincter muscle is now well developed. The ciliary body has almost completely developed by this time as well. The pupillary membrane extends over the entire surface of the iris and forms the superficial vasculature of the iris. By the end of the sixth month the vessels of the pupillary membrane start to atrophy. The angle of the eye now contains the differentiated structures of the adult eye: scleral spur, trabecular meshwork, Schlemm's canal and an iris (Figure 11). The apex of the angle is positioned even with the middle area of the ciliary processes while some of the processes have moved posteriorly to the apex of the angle. The ciliary processes eventually all become located posterior to the angle apex. The cell surface area of the trabecular meshwork exposed to the angle increases while the intercellular cytoplasmic connections of the trabecular meshwork cells continue to grow in number.

Development of the anterior segment during the seventh month is quite active in comparison to month six. The iris undergoes several changes: the sphincter muscle develops what appear to be interdigitations that indicate cell to cell conduction. The

Figure 11. Detail of mature anterior angle chamber. By the sixth month of development the rudiments of the final structures of the angle are in place (Adapted from (3)).

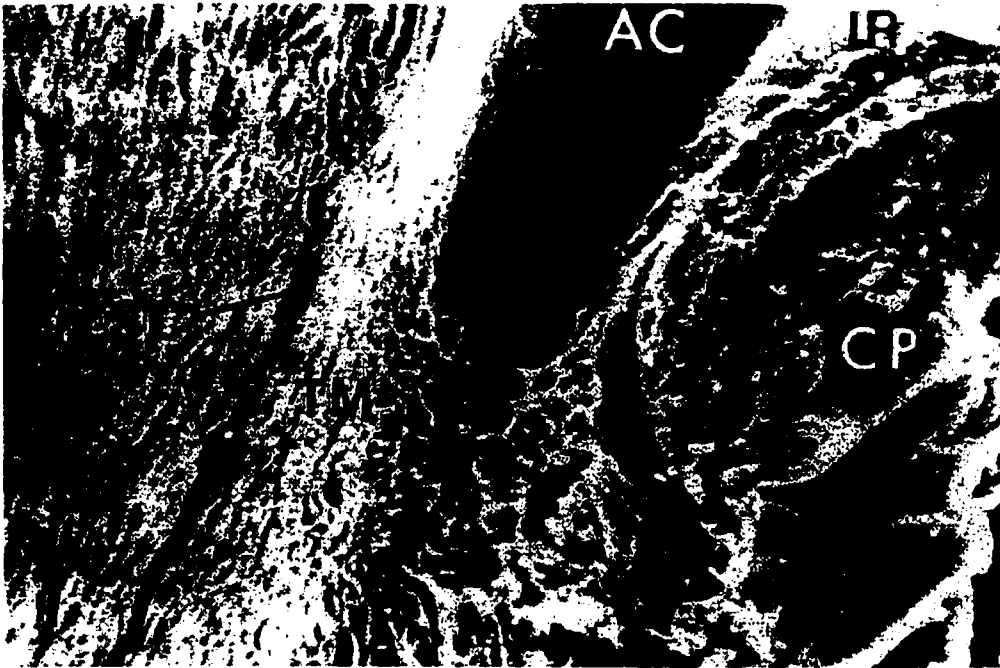


posterior layer of the iris becomes further pigmented and the marginal sinus disappears. The vascularization of the iris stroma through the pupillary membrane continues to atrophy. It is also at this time that the Hyaloid artery starts to shrink and lose blood flow (Figure 7). During the seventh month the angle structure continues to develop. The apex of the angle moves farther to the posterior of the eye due to what is thought to be differential growth between the periocular mesenchyme and the anterior neuroectoderm (1, 2). The periocular mesenchyme grows at approximately three times the rate of the anterior neuroectoderm with the result that the apex of the anterior chamber angle is now placed near the middle of the trabecular meshwork (1, 2) (Figure 12). The ciliary processes also assume their final placement posterior to the angle and the major arterial circle of the iris also moves to a location posterior to Schlemm's canal. Programmed cell death is thought to be a key part of the remodeling of the anterior chamber at this time as apoptotic cells are thought to be present near the trabecular meshwork, iris root, ciliary body and the nearby choroid structures (1, 2). It is possible that cell death could also be part of the development of the spaces in the trabecular meshwork (1, 2, 3).

The eye develops quite slowly during the eighth and ninth months. Corneal development continues, including a thickening of Descemet's membrane with the final characteristics of the cornea present at the time of birth. Iris development continues slowly during the final stages of pregnancy. The sphincter muscle becomes free of the posterior mesenchyme and is well developed by the time of birth. The dilator pupillae continues to develop. The minor arterial circle of the iris is well formed by nine months and the deposition of collagen in the anterior stroma of the iris is progressing. The apex of the angle continues to move more posteriorly through the eighth and ninth months and at birth it is positioned posterior to Schlemm's canal (1, 2) (Figure 12).

At birth the eye is almost completely developed. The iris is still quite flat and has only a thin stroma. After birth, crypts form on the iris surface. The colour of the iris

Figure 12. Scanning electron micrograph of an angle at 7 months of development. Figure indicates position of angle in relation to iris (IR), ciliary process (CP) and trabecular meshwork (TM). SC refers to Schlemm's canal. AC refers to the anterior chamber. (Adapted from (1)).



changes due to melanocytes in the stroma producing pigment. This colour change continues for approximately six months postnatally. (1, 2). The angle of the anterior chamber is open at the time of birth but deepening of the angle continues for several years after birth and the angle recess appears (Figure 13). The trabecular meshwork also undergoes a remodeling for sometime after birth. More gaps appear between the cytoplasmic extensions of the trabecular cells (1, 2).

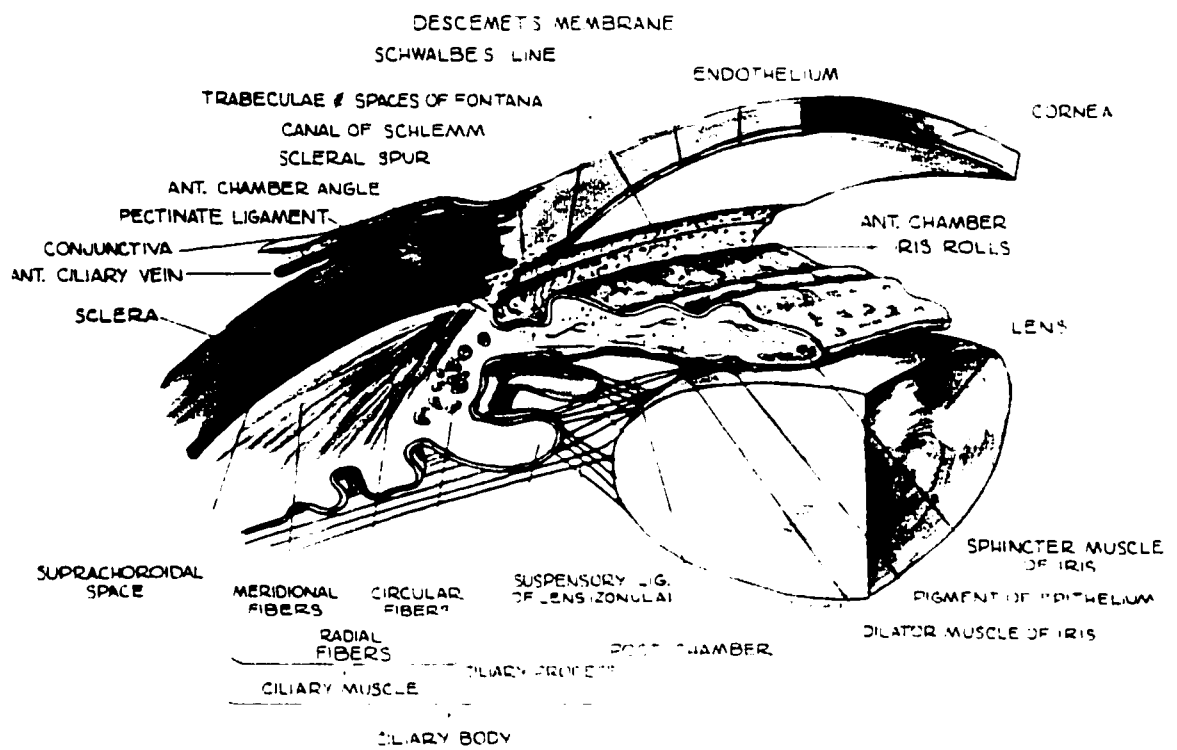
If all the steps of eye development have occurred at their proper time for the proper duration and at the proper place then the eye should be structurally functionally normal (Figure 13). However, the complex cascade of steps needed to produce a normal human eye occasionally fails to proceed properly. Glaucoma is one possible result of developmental disruption.

Glaucoma

Glaucoma is a disease process resulting in damage to the fibers of the optic nerve and, if untreated, blindness. One of the main risk factors for developing glaucoma is increased pressure of fluid inside the eye (intraocular pressure or IOP). The increased pressure in the eye is transferred to all tissues inside the eye including the optic nerve. It is thought that the increased pressure present in the globe of the eye distorts and bends the neuronal axons of the optic nerve. This causes a slow atrophy and cell death, leading eventually to loss of vision (3). Glaucoma is the second leading cause of blindness in persons over 50 years of age in North America and the World Health Organization estimates 66.8 million cases of glaucoma world wide by the year 2000 (4).

In order to understand the pathology of glaucoma it is necessary to understand the normal regulation of pressure inside the eye.

Figure 13. Diagram of mature anterior chamber of the human eye (Figure courtesy of M. Walter).

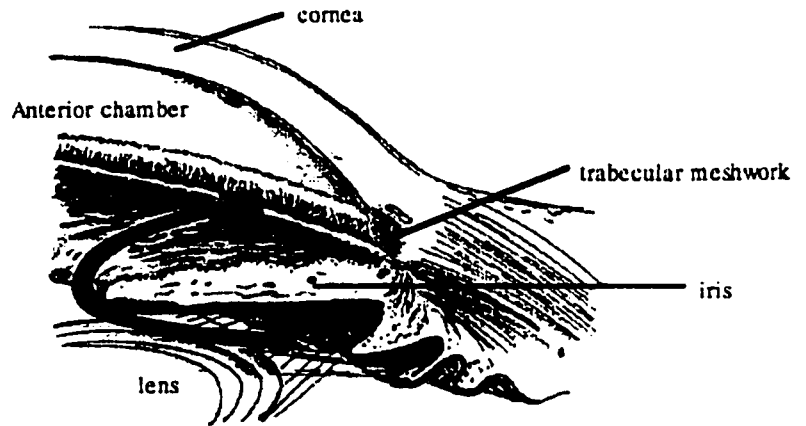


The aqueous humor that fills the eye is produced by the ciliary process located just posterior the iris (Figure 13). This fluid needs to be removed from the eye in order to prevent the pressure inside the eye from rising. The usual drainage route of the aqueous humour is through the anterior chamber, exiting the eye through the trabecular meshwork and into Schlemm's canal (3) (Figure 12). The fluid is then drained into the lymphatic circulation (3). Blockage of this outflow of aqueous humour is one of the principal causes of increased pressure in the eye leading to glaucoma. Glaucoma can be categorized into three broad groups: open and closed angle glaucoma and congenital glaucoma (3). As the names indicate the characteristic differentiating factor between the open and closed angle categories of glaucoma depends upon the structure of the angle of the anterior chamber. Closed angle glaucoma results when the angle of the eye becomes physically blocked in such a way that the aqueous humour produced by the ciliary process cannot drain out of the eye. In open angle glaucoma the angle of the anterior chamber is physically open, but for some reason is unable to allow adequate passage of fluid out of the eye. As a result the fluid pressure in the eye rises (3) (Figure 14)

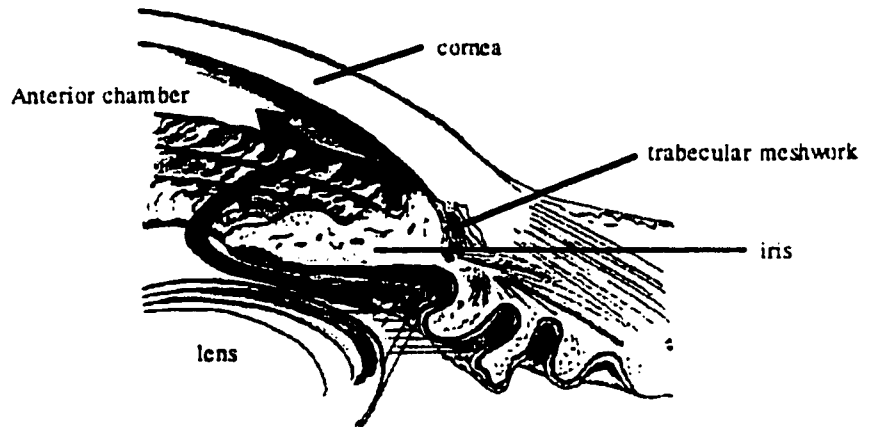
In addition to the differentiation of glaucoma based on angle structure, glaucomas are also classified based upon their etiology. Primary glaucomas results from some disturbance in the anterior segments of the eye responsible for the outflow of the aqueous humour (3). No other ocular or non-ocular system is involved in primary glaucoma (3). Secondary glaucoma, however, results when some underlying ocular or systemic event predisposes the eye to the development of glaucoma (3). The congenital classification of glaucoma applies when a patient is born with glaucoma already present. Under these definitions for primary and secondary glaucoma, developmental defects which result in the subsequent appearance of glaucoma are classified as secondary, or developmental glaucoma (3).

Figure 14. Diagram illustrating the structural difference between open and closed angle glaucoma. Arrows indicate direction of flow in open and closed angles (Diagram courtesy of Dr. I. MacDonald).

Open-angle
glaucoma



Angle-closure
glaucoma



One particular developmental eye disorder which frequently present with glaucoma is Axenfeld-Rieger anomaly and syndrome (ARA and ARS) and Iridogoniodysgenesis anomaly and syndrome (IGDA and IGDS). All of these conditions result from developmental abnormalities of the anterior segment of the eye. ARA, ARS, IGDA, and IGDS all present with an open anterior angle of the eye and are therefore all classified as secondary open angle glaucoma.

History of Axenfeld-Rieger and Iridogoniodysgenesis Syndromes

Axenfeld in 1920 first described a patient with a prominent annular white line near the limbus at the level of Descemet's membrane (*embryotoxon posterior*) (5). Rieger in 1934 described two patients with findings noted by Axenfeld but also observed iris stromal atrophy and congenital pupillary abnormalities (ectopia, dyscoria) (Figure 15 A) (6). Subsequently, Rieger in 1935, considered the *embryotoxon posterior* and iris hypoplasia to be features of a single disorder that he termed *dysgenesis mesodermalis corneae et iridis* (7). Some of the patients with this disorder had associated non-ocular developmental defects, particularly involving the teeth, facial bones and periumbilical skin (Figure 15 B) (8, 9). The similarity of anterior segment angle defects described by Axenfeld and Rieger has led to the suggestion that these findings are part of a spectrum of developmental disorders (3, 7). Patients with ARA present with the characteristic ocular features alone, while the phenotype showing both ocular and non-ocular features is classified as ARS (3) (Table 1). Glaucoma occurs in approximately half of ARA and ARS cases (3).

Iridogoniodysgenesis (IGD) is a related ocular malformation characterized by abnormalities in the differentiation of the iridocorneal angle tissue (goniodysgenesis) and

Table 1: Characteristic ocular and non-ocular phenotype of Axenfeld-Rieger Anomaly and Syndrome (ARA/ARS) and Iridogoniodysgenesis Anomaly and Syndrome (IGDA/IGDS). “*” hearing loss has been reported in one family with ARS symptoms (13).

Ocular	ARA	ARS	IGDA	IGDS
Iris Hypoplasia	+	+	+	+
Displaced Schwlabe Line	+	+	-	-
iris adhesions	+	+	-	-
pupil abnormalities	+	+	-	-
Goniodysgenesis	+	+	+	+
Glaucoma/IOP	+	+	+	+
Non-ocular				
Dental anomalies	-	+	-	+
Maxillary hypoplasia	-	+	-	+
Umbilical defects	-	+	-	+
Hearing Loss	-	+*	-	-

maldevelopment of the anterior stromal layer of the iris associated with increased intraocular pressure resulting in juvenile glaucoma (Figure 15 C) (10, 11). IGD was first recognized by Berg in 1932 as an autosomal dominantly inherited disorder (12). Jerndal later re-examined and expanded Berg's pedigree and confirmed iris and iridocorneal angle defects characteristic of IGD (14). Weatherill and Hart, in examining a different family, found iris hypoplasia and iridocorneal angle defects in 30 affected individuals (15). These latter two studies established the slit lamp and gonioscopic features of the iris and anterior chamber angle abnormalities upon which rests the current understanding of IGD. Some IGD patients have associated non-ocular developmental defects in the teeth, facial bones, and periumbilical skin (Figure 15 D) (11). In a manner analogous to that observed in patients with Axenfeld-Rieger eye malformations, patients with Iridogoniodysgenesis anomaly (IGDA) present with the characteristic ocular features alone; the phenotype seen in patients with both IGD ocular and non-ocular features is classified as Iridogoniodysgenesis syndrome (IGDS). Between 75 and 100% of IGD patients develop glaucoma (16).

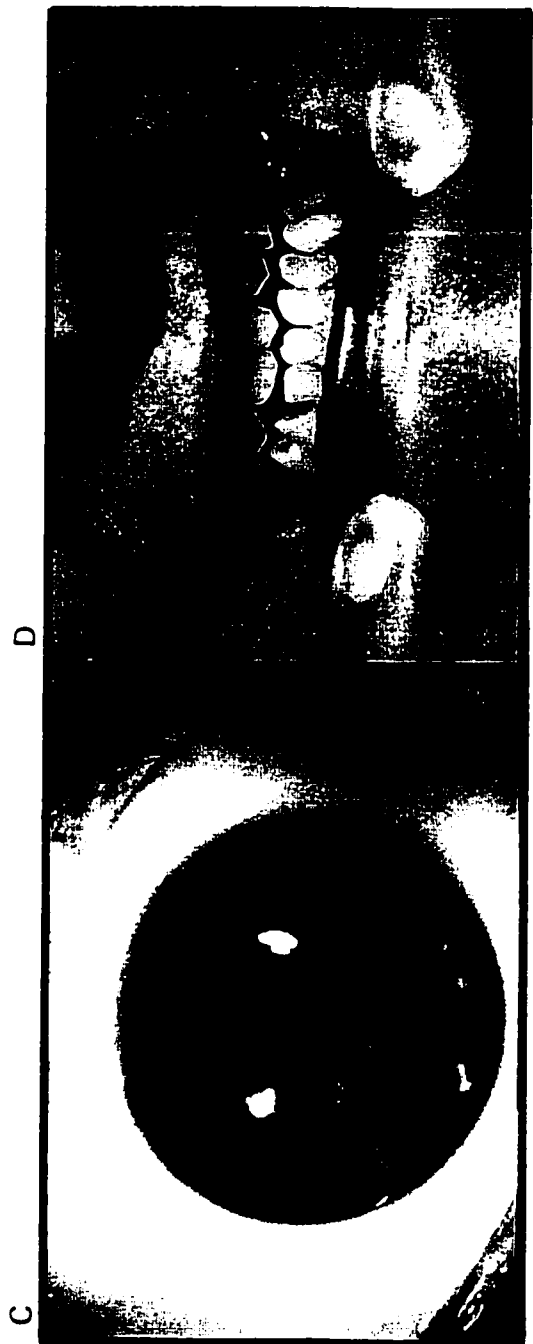
As research into eye development continues, more genes are being isolated which, when mutated, have been shown to be responsible for the development of glaucoma. Many of these "developmental glaucoma" genes are thought to be necessary for the normal development of the eye and belong to a class of genes that encode transcription factors.

Figure 15 A. The eye of an individual affected with ARS. Note the full thickness tears and displaced pupil. Also, the anteriorly displaced Schwalbe line is visible in the left hand side of figure. (Photo courtesy of Dr. M. Walter)

Figure 15 B. Illustration of the missing and misshapen teeth typical of ARS. (Photo courtesy of Dr. M. Walter)

Figure 15 C. The eye of an individual affected with IGDS. Notice that the iris in this individual is hypoplastic but otherwise unremarkable. No tears in the iris stroma are visible and there is no appearance of a displaced Schwalbe line. The pupil appears normal in size and position. (Photo courtesy of Dr. M. Walter)

Figure 15 D. Illustration of the missing and misshapen teeth typical of IGDS. (Photo courtesy of Dr. M. Walter)



Transcription factors and Eye Development

The development of the human eye is extremely complex and requires the coordinated activity of many genes. A large number of the genes necessary for eye development can be classified as transcription factors. Transcription factors are proteins which can activate or repress other genes usually by binding to DNA near these target genes thereby regulating their expression (54). In this way, transcription factors turn on and off the "switches" (genes) which direct the development of multicellular organisms.

There are many transcription factors known to be involved in the development of the eye (4, 17-21). PAX6, PAX2, and CHX10 are examples of other transcription factors involved in eye development and will also be discussed. The most relevant example to this study is the RIEG1/PITX2 gene which is the focus of this work.

RIEG1/PITX2 is a member of the *bicoid* class of homeobox containing transcription factors. The bicoid group is defined by a lysine residue located at residue nine of the third helix of the homeobox. RIEG1/PITX2 was cloned in 1996 by Semina and co-workers (21). The gene is located at chromosomal band 4q25, a region which has long been known to be linked to ARS (22). The gene for RIEG1/PITX2 spans approximately 18kb of genomic DNA and is comprised of 4 exons of 572, 57, 206 and 1290 nucleotides in length. The RIEG1/PITX2 homeobox is split by the intron between exons 3 and 4. The initiating (ATG) codon is located in exon 2 and the terminating TGA codon is situated in exon 4. The discovery of mutations in the RIEG1/PITX2 gene in patients affected with ARS, and the Rieg1/Pitx2 expression profile in the mouse in tissues affected by ARS, such as the developing eye cup, maxillary process and umbilicus, argue strongly in favour of RIEG1/PITX2 being the gene responsible for ARS (21) (Figure 16 and Figure 17). Other key genes involved in eye formation include CHX10, PAX2, PAX6

Figure 16. PITX2 gene indicating key domains, transcription start and stop sites and location of PCR primers used to amplify sections of the PITX2 gene (23).

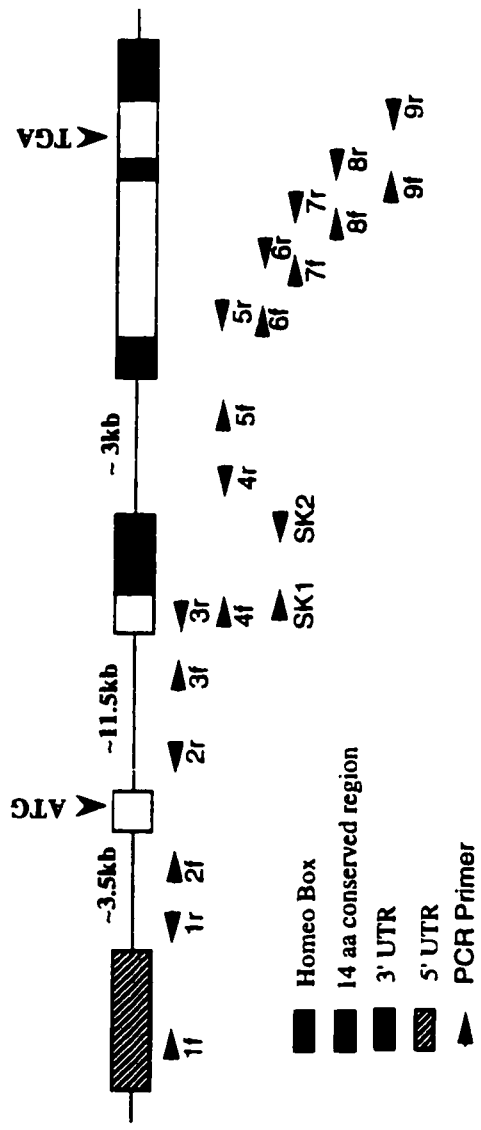
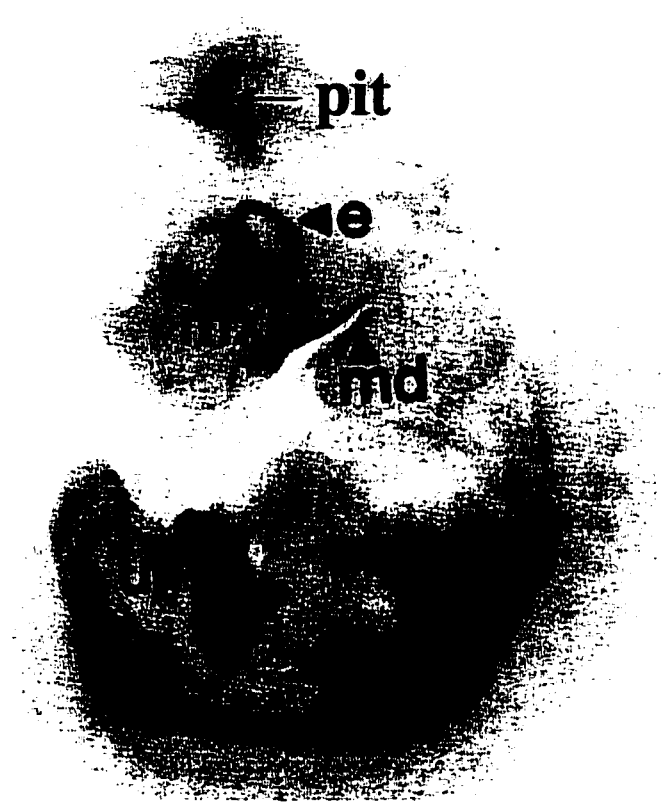


Figure 17. Expression of the Pitx2 gene in embryonic mouse. Demonstrates that the Pitx2 gene is expressed in the tissues affected in ARS patients. E = eye, mx = maxilla, md = mandible, u = umbilicus, l = limb, pit = pituitary gland (From 21).



and FKHL7. All four of these genes, like PITX2, encode transcription factors, mutations of which cause a wide range of eye malformations.

Chx10 is a member of the paired class of homeodomain proteins and is expressed most predominately in the developing and mature retina (17). As with most eye related transcription factors, Chx10 is also expressed in the developing central nervous system including the thalamus and ventral spinal cord (17). Mutations in Chx10 manifest themselves in a autosomal recessive phenotype in the mouse called ocular retardation (*or*) (17). This *or* phenotype comprises numerous eye malformations including microphthalmia, thin retina, optic nerve hypoplasia, and an absence of differentiated bipolar cells (17).

PAX genes encode a class of transcription factor originally isolated from a *Drosophila* segmentation mutant referred to as *paired* (24, 25). The common DNA binding domain in these transcription factors is a 128 amino acid stretch which contains two DNA binding domains. These two binding domains appear to be two homeobox domains arranged in tandem. (24, 25). In addition to the paired box observed in PAX genes, some members of the PAX family also contain a homeobox DNA binding motif (24, 25). PAX genes have been isolated from many types of multicellular organisms including *Drosophila*, Zebrafish, chicken and human (26). To date, nine members of this family are known to exist in humans and all play significant roles in the development of the human body plan. Two of the PAX genes known to be involved in eye development are PAX2 and PAX6 (17).

PAX2 is expressed in the brain, spinal cord, optic stalk, kidney, and hindbrain. Mutations in PAX2 can affect both the eye and the kidney resulting in renal and optic colobomas (27).

PAX6 is currently the best understood of the transcription factors involved in eye development. PAX6, as the name denotes, is also a member of the paired box class of transcription factors, but in addition to the paired box, PAX6 also contains a complete

homeobox downstream of the paired box (17). PAX6 is expressed throughout the developing eye in many cell types and has a large influence over the formation of the eye (17). PAX6 expression is initially seen in the optic vesicle, optic stalk, and lens ectoderm. As development progresses, PAX6 expression appears in corneal ectoderm, throughout the lens, the neuroretina as well as the brain and spinal cord.

PAX6 mutations cause a wide variety of eye malformations in many different organisms. In humans, PAX6 has been shown to be mutated in cases of aniridia, Peter's anomaly, autosomal dominant keratitis, and anterior segment anomalies (28, 29, 30, 31). Heterozygous mouse mutants of PAX6 present with the *smalleye* phenotype while *Drosophila* homozygous mutants in PAX6 present with the *eyeless* phenotype (17). Homozygous PAX6 mutants in mice present with a complete absence of eye and nasal structures and forebrain (32) while the one identified human PAX6 homozygote presented with absence of eyes, severe craniofacial dysmorphism, and large scale disturbances in the formation of the brain and spinal column (33). Ectopic expression of the mouse PAX6 gene in the imaginal discs of *Drosophila* embryos directed the formation of what appeared to be normal looking *Drosophila* eyes in tissues where eyes are not supposed to form, such as the tips of the antennae (34). This work clearly showed that PAX6 is a highly conserved gene playing a major role in the formation of the eye in highly divergent species.

The FKHL7 gene at 6p25, another gene involved in eye development, has recently been cloned. This gene codes for the production of a transcription factor shown to belong to the *forkhead* domain family. Mutations in FKHL7 can result in both the ARA phenotype (35, 36) and the ARS phenotype (77). The fact that a single eye disorder can be caused by mutations in different genes (locus heterogeneity) may pose difficulties when and if genetic screening is performed on families in which an eye malformation is segregating. In order to assess carrier or affected status of an individual, many different genes may have to be examined.

My graduate studies work entailed a detailed mutational analysis of the RIEG1/PITX2 gene in 14 families that display ARS-like symptoms. My objectives were to: 1) determine the frequency of ARS cases caused by mutations in the RIEG1/PITX2 gene and 2) to ascertain whether any phenotype/genotype correlations exist between RIEG1/PITX2 mutations and the resulting eye phenotype.

Materials

6% Sequencing Gels

40.5g Urea
40ml distilled water
4.5ml 20X GTB buffer
13ml 40% Acrylamide/Bis-acrylamide (19:1)

20X GTB Buffer

54g TRIS Base
18g Taurine
1g Na₂EDTA · 2H₂O
250 ml distilled water

SSCP Non-denaturing gels

58.5 mls distilled water
9 ml 10X TBE buffer
9 ml 100% Glycerol
13.5 ml 40% Acrylamide/Bis-acrylamide (19:1)

Red Cell Lysis Buffer

4.12g TRIS Base
14.9g Ammonium Chloride
Deionized water to 2000ml, final pH adjusted to 7.65

White Cell Lysis Buffer

40 mL of 0.5 mol/L EDTA pH 8.0
50 mL of 1 mol/L TRIS
100 mL of 5mol/L NaCl
Deionized water to 500mL, final pH adjusted to 8.0
Autoclave and then add 5 mL of 20% SDS.

0.15 mol/L NaCl

120 ml 5 mol/L NaCl
Deionized water to 4000mL. Autoclave.

High TE Buffer

100 mM TRIS base
40 mM EDTA pH 8.0

4 mol/L Ammonium acetate

30.8 g Ammonium acetate
Deionized water to 100mL
Sterilize by filtration

10X TBE Buffer

108 g TRIS Base
55 g Boric Acid
40 ml 0.5M EDTA
1L distilled water

Denaturing Solution

0.5 M NaOH
1.5 M NaCl

Neutralizing Solution

0.5 M TRIS pH 7.5
1.5 M NaCl

Low Stringency Wash Solution

2X SSC, 0.1% SDS

High Stringency Wash Solution

0.2 X SSC, 0.1% SDS

Church and Gilbert Hybridization solution:

24.3 g Na_2HPO_4
10.9 g $\text{NaH}_2\text{PO}_4\text{H}_2\text{O}$
35.0 g SDS
5.0 g BSA (fraction V)
ddH₂O to 500mL total volume.

Restriction Enzyme buffer for EcoRI Genomic Digests

50 mM NaCl
100 mM Tris-HCl
10 mM MgCl₂
0.025% Triton X-100
pH 7.5 at 25°C

Methods

Patients:

Patients willing to participate in the PITX2 mutational study were referred to us by consulting physicians. A detailed description of the phenotype of each patient is presented in Table 2. Patients were diagnosed with Axenfeld-Rieger syndrome by current criteria which include iris hypoplasia, adhesions between the iris and cornea, anomalous anterior angle vascularity, extra tissue in the irido-corneal angle, increased intraocular pressure, anteriorly displaced Schwalbe line, dental anomalies, and umbilical anomalies (37). The ADA family, presenting with IGDS and not ARS (see Table 2), has previously been genetically linked to chromosome 4q25. Since this is the chromosomal location of the PITX2 gene shown previously to be associated with some cases of ARS (21) this family was also included in my screen of the PITX2 gene.

Participation and consent of each patient involved was approved through the University of Alberta Research and Ethics Board.

Table 2: Phenotypic Characteristics of Patients in PITX2 Study.

<u>PHENOTYPE</u>	<u>INDIVIDUALS</u>														
	OCULAR	CM	JD	MF	LS	AH	AG	KR	KR'	DD	MC	DG	MP	GL	BK
Iris Stromal Hypoplasia	+	+	+	+	+	?	+	+	+	+	+	+	-	+	
Posterior embryotoxon	+	+	-	-	-	?	+	+	?	+	-	-	?	+	
Iris processes	+	?	-	+	-	?	+	+	?	+	-	+	+	+	
Pupillary anomalies	+	+	+	+	+	+	-	+	+	+	-	-	-	+	
Elevated IOP/Glaucoma	+	+	+	+	-	+	?	+	+	+	+	+	+	+	
Abnormal Angle	-	?	+	+	+	?	+	-	?	?	+	-	-	-	
Anterior TM insertion	-	+	+	+	-	?	-	?	?	?	+	?	+	?	
Abnormal blood vessels	+	+	-	-	-	?	-	?	?	?	-	?	-	-	
Abnormal angle tissue	-	?	+	+	-	?	-	+	?	?	-	?	-	+	
NON-OCULAR															
Dental anomalies	+	?	-	?	-	+	?	+	?	?	+	?	-	+	
Maxillary hypoplasia	+	+	-	?	-	+	?	+	?	-	+	?	-	+	
Abdominal anomalies	-	?	?	?	-	?	?	+	?	?	+	?	-	-	
<u>DIAGNOSIS</u>	ARS	ARS	IGDA	ARA	UNK	ARS	ARA	ARS	IGDA	ARA	IGDS	IGDA	IGDA	ARS	

Individuals were assessed by qualified ophthalmologists in regards to signs of Axenfeld-Rieger syndrome. Individual DG, from the ADA family, presented with IGDS and was included in this study as linkage analysis indicated the IGDS phenotype in the ADA family was linked to the PITX2 region (38). A "+" sign indicates that the trait is present in an individual while a "-" sign indicates that the trait is not present. A "?" indicates uncertainty as to the presence of the trait in that individual. ARA refers to Axenfeld-

Reiger Anomaly. ARS refers to Axenfeld-Rieger Syndrome. IGDA refers to Iridogoniodysgenesis Anomaly. IGDS refers to Iridogoniodysgenesis Syndrome. A diagnosis of "UNK" refers to eye findings which do not fit the standard criteria for AR or IGD including optic nerve hypoplasia and cataracts.

Genomic DNA

DNA was purified from whole blood lymphocytes using standard lysis/phenol extraction protocols (38, 39). Whole blood was centrifuged for five minutes at 2000 rpm and 4°C. The plasma supernatant and red blood cells were discarded while the buffy coat was transferred to a fresh 15ml polypropylene tube. 20 mls of RBC lysis solution was added followed by up to 5 minutes in a 37°C water bath until red cells were lysed. This was monitored by the change of the solution from cloudy red to clear red. The cells were then centrifuged at 2000 rpm/4°C for ten minutes. The supernatant was then discarded leaving a pellet of white blood cells. The pellet was then washed in 25 ml of 1.5M NaCl and then centrifuged as above. The supernatant was again discarded and the white cells resuspended in 2mls of High TE buffer. White cells were then mixed with an additional 2mls of white cell lysis buffer and stored at 4°C overnight. The lysed white blood cells were then extracted with an equal volume of buffer saturated phenol for 20 minutes at room temperature followed by centrifuging at 2000rpm at room temp for 10 minutes. The supernatant was moved to a fresh tube and extracted with phenol one more time and then twice with chloroform/isoamyl alcohol (24:1) under the same conditions. The final supernatant was removed and mixed with 400µL of 4M ammonium acetate and 40mls of 95% ethanol to precipitate the genomic DNA. The genomic DNA was stored at -20°C overnight. The pellet of DNA was then rinsed in 70% ethanol and resuspended in 400µL sterile distilled water. DNA was analyzed spectrophotometrically to determine concentration and purity prior to further manipulations.

PCR Amplification

PCR amplification of the coding sequence and intron exon boundaries of the PITX2 gene was carried out using standard procedures. Primer sequences were

graciously provided by E.V. Semina and Jeff Murray at Iowa State University, Iowa City, Iowa U.S.A. Primer set 3aF and 3aR were designed to amplify an alternately spliced exon of PITX2 detected by Gage and Camper (40). Two additional primers SK1 and SK2 were designed using the Whitehead Institutes Primer 3 design program accessed via the World Wide Web at www.genome.wi.mit.edu/cgi-bin/primer/primer3.cgi. Standard PCR reactions were prepared as follows: 2.5 μ L of 10X buffer, 2.5 μ L of 2mM dNTP mix, 1.5 μ L 25 μ M MgCl₂, 0.05 μ g of relevant primers, 0.125 μ L of 100X acetylated BSA, 25ng of template DNA, 10 units of *Taq* polymerase and sterile distilled water as needed to bring final volume to 25 μ L. Primers were produced by the Biochemistry DNA Synthesis lab at the University of Alberta or from Gibco/BRL Life Sciences as needed. See Table 3 and Figure 16 for information on the primer pairs used to amplify the various sections of the PITX2 gene. An exception to the standard PCR reactions above was performed with primer pair SK1 and 4R. This primer pair was used to span the region of the PITX2 gene where the mutation present in the ADA family was discovered. Initially the ADA mutation was found by sequencing the 4F/R PCR product. Reproduction of the 4F/R PCR reaction proved difficult so primers SK1 and SK2 were designed to span the mutation in the ADA family. SK1 and SK2 also proved to give inconsistent results. In an attempt to solve the dilemma, SK1 and 4R were used together in a "touchdown" PCR reaction to accommodate the difference of 5 $^{\circ}$ C in the annealing temperatures between SK1/4R. The conditions for the SK1/4R "touchdown" PCR reaction are as follows: denaturing at 95 $^{\circ}$ C for 5 minutes, 95 $^{\circ}$ C for 30 seconds, with an initial annealing temperature of 55 $^{\circ}$ C for 30 seconds and an extension reaction of 72 $^{\circ}$ C for 1 minute. The annealing temperature was ramped down by 0.5 $^{\circ}$ C per round of PCR for 10 rounds ultimately resulting in an annealing temperature of 50 $^{\circ}$ C. A further 35 rounds of PCR were then carried out as usual using the 50 $^{\circ}$ C annealing temperature.

PCR Product Purification

Prior to sequencing, PCR products were purified using Qiagen columns (Qiagen Corporation) according to the manufacturer's instructions. Samples were either isolated on 1% agarose/ethidium bromide gels and then purified, or purified directly from the PCR reaction mix after a sample was checked on a gel for purity and proper size of product.

Sequencing

Purified PCR products were sequenced using the Amersham ³³P Thermosequenase kit (Amersham Life Sciences). Twenty-five rounds of cycle sequencing were carried out as follows: 95°C denaturing for 30 seconds, annealing at the temperature specific to the primer being used (see Table 3) for 30 seconds, and 72°C extension for one minute. Products were separated on 6% denaturing acrylamide gels for 1.5 to 3.5 hours (depending on product size) at 60W power and visualized by autoradiography on Kodak Biomax film.

SSCP Analysis

SSCP reactions were carried out following the PCR amplification protocol above with the addition of 5μCi ³⁵S-dATP (1000μCi/ ml) and a reduction of unlabeled dATP to 0.25mM from 2mM (30). PCR products were separated on 6% acrylamide gels with 10% glycerol for 8 hours at 4°C and 60W, prior to visualization by autoradiography.

Table 3 PCR Primers used to amplify sections of the PITX2 gene.

Primer Pair	Annealing Temp(°C)	Sequence 5' to 3'	Size (bp)
1 F/R	55°C	F-cgtggactccttcggaactt R-ccagactcgcattatctcac	~180
2 F/R	56°C	F-ctgaagcctagcacacagta R-gcaggagaaggggttctta	~200
3 F/R	56°C	F-cagctcttcacggcttet R-gcggcccagctctcattctt	~100
4 F/R	56°C	F-gataaaagccagcaggggaa R-cttccacattctctctggt	~280
5 F/R	56°C	F-gtaatctgcactgtggcattc R-ccagttgtaggaatagcc	180
6 F/R	56°C	F-agttcaatgggctcatgcag R-ggggaaaacatgctctgtga	150
7 F/R	55°C	F-gcttcccccttttcaactet R-ggctactcaggttcttcaag	174
8 F/R	56.5°C	F-actctatctgctccatgagc R-caggctcaggttacacgtgt	201
9 F/R	62°C	F-gccgactcctccgtatgttt R-ctgtgggtcggctcaca	170
SK1 F/R	55°C	F-accctcttaagaagaagcgg R-gcttccgtaaggttgctcc	240
3a F/R	56°C	F-acgcctctctccgcacgt R-ttcttgcgctttcggccga	280

Marker Analysis

Three families (A, B, and C) (Figure 18, 19, 20) that showed no mutation of the PITX2 gene were large enough to be useful in linkage studies. Family A is a four generation family with DNA samples available from twenty people including eighteen children of affected individuals. Family B is a three generation family with DNA available from fifteen individuals and DNA from thirteen children of affected individuals. Family C is a four generation family with DNA available from twenty-seven individuals and DNA from ten children of affected individuals. Markers D4S2623 and D4S1652, flanking the PITX2 gene, were used to detect linkage to the PITX2 gene. Markers D13S1297 and D13S1253 are on chromosome 13 in the 13q14 region for which linkage has been demonstrated for some cases of ARS (13). Markers D6S344 and D6S1600, flanking the FKHL7 gene, were used to check for linkage to 6p25. Marker D11S907 was used to examine possible linkage to PAX6. The primers for these markers were supplied by Research Genetics Inc. or GIBCO/BRL Life Sciences. Genomic DNA from the family members (prepared as previously described) was diluted to approximately 50 ng/ μ L prior to PCR reactions. PCR conditions for the amplification of markers followed conditions for SSCP reactions at an annealing temperature recommended by the primer supplier. Products were denatured at 95°C for 5 minutes and then quick cooled on ice prior to loading on 6% gels as used for electrophoresis of DNA sequencing products. Visualization was performed using Kodak Biomax film exposed at room temperature.

Figure 18. Pedigree of Family A. Asterisks refer to patients for whom DNA is available. The + sign indicates person whose DNA was sequenced in the PITX2 mutation screen.

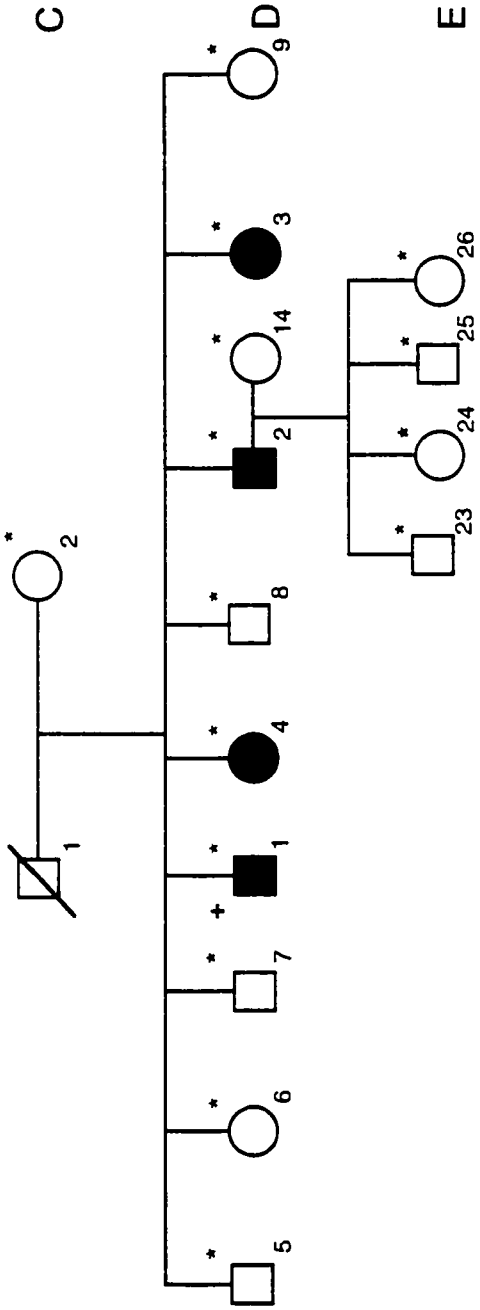


Figure 19. Pedigree of Family B. Asterisks refer to patients for whom DNA is available. The + sign indicates person whose DNA was sequenced in the PITX2 mutation screen.

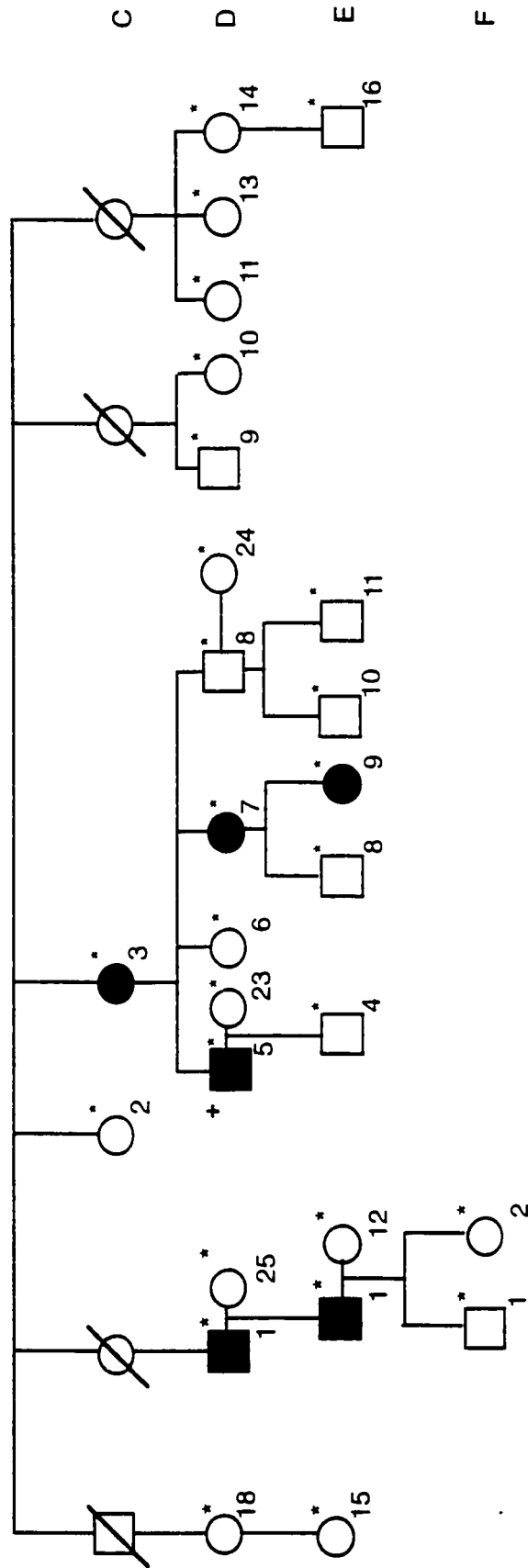
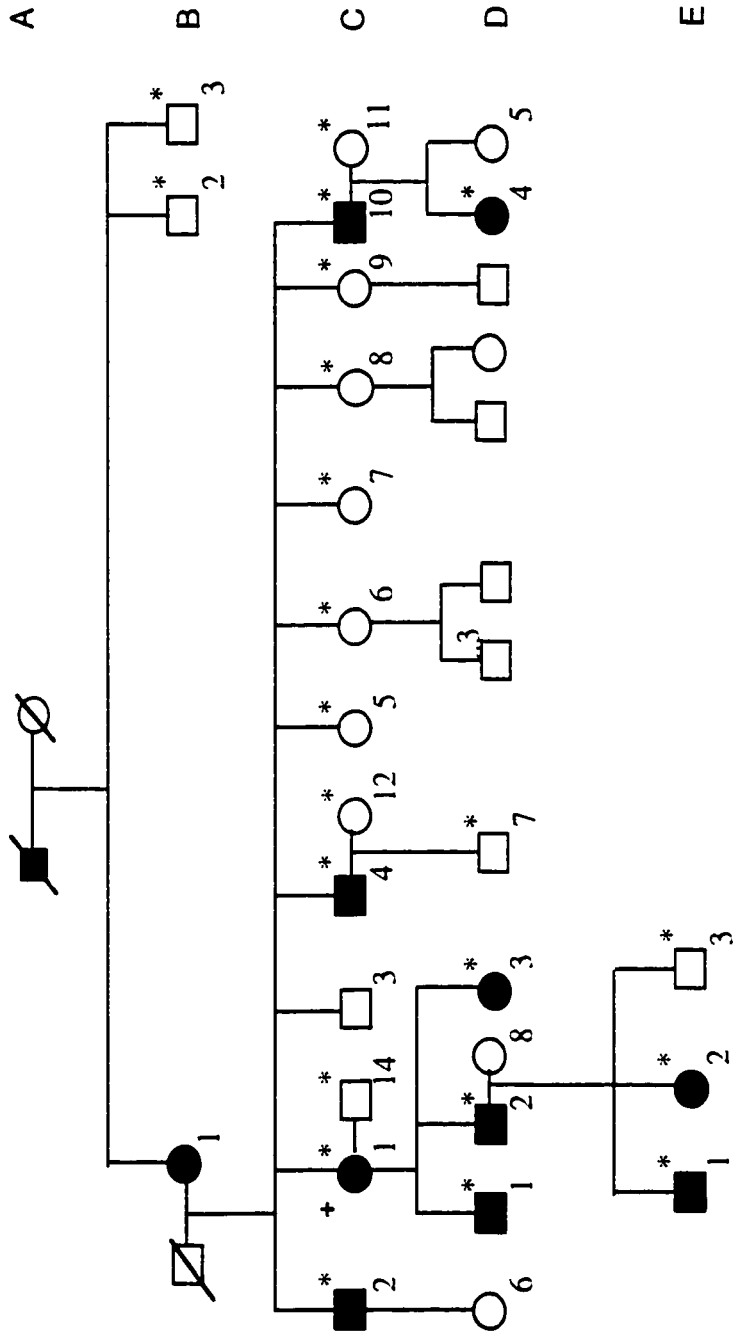


Figure 20. Pedigree of Family C. Asterisks refer to patients for whom DNA is available. The + sign indicates person whose DNA was sequenced in the PITX2 mutation screen.



Linkage Analysis

Marker data was stored and exported for each family using the hypercard-based program LINKAGE INTERFACE (41, 42, 43) on a DOS-compatible Power Macintosh 6100/66 computer (Apple computers, Inc, Cupertino, CA). Data analysis was carried out using the MLINK option of the DOS-computer linkage analysis program LINKAGE. A LOD score of over 3 was considered significant evidence of linkage while a LOD score of -2 was considered exclusion of linkage according to Morton's criteria (44).

Southern Blots

A genomic Southern blot was performed to determine if the ARS phenotype in families where no mutation in PITX2 had been detected was due to a microdeletion. Total genomic DNA was digested with the restriction endonuclease *EcoRI* for 8 hours at 37°C in standard buffers. The digestion was carried out as follows: 3µg of total DNA with 10 units *EcoRI* enzyme and 2µL (10X) buffer plus sufficient water to take the final reaction volume 20µL. After 4 hours of the 8 hour digestion a further 10 units of enzyme was added to ensure complete digestion of the genomic DNA. The genomic DNA was electrophoresed in a 1% agarose gel for 4 hours at 100 volts. The gel was soaked twice for 20 minutes in denaturing solution and twice for 20 minutes in neutralizing solution. Transfer of the DNA to Hybond N membrane (Amersham Life Sciences) was carried out overnight using standard transfer apparatus. Following transfer, the membrane was baked for 2 hours at 80°C under vacuum.

Probes for Southern

Probes were prepared using Gibco/BRL Life Technologies Random Primer labeling kit. The DNA used was either the PITX2 full length cDNA or the FKHL7 full length cDNA (as a control). Probe DNA (25 to 50 ng) was heat denatured for 5 minutes at 95°C and then quick cooled on ice for five minutes. The DNA was then mixed with 2µL reaction buffer, 6µL hexanucleotide random primers, 5µL ³²p-dCTP, 10 units Klenow enzyme and sufficient water to make the final reaction volume 20µL. The labeling reaction was incubated for 2 hours at 37°C. After labeling, the probe was denatured at 95°C for 5 minutes and quick cooled on ice prior to addition to the hybridization solution.

Hybridization of probes to Southern Blot

Genomic Southern blots were prehybridized in 10mL of Church and Gilbert hybridization solution for 4 hours at 65°C (45). Probes were denatured at 95°C for 5 minutes and then quick cooled on ice prior to being added to the hybridization solution. Hybridization of the probe was carried out overnight at 65°C. The following day the membrane was washed twice for 20 minutes at 65°C in low stringency wash. The membrane was checked by scanning briefly with a Geiger counter. If the membrane was judged to be clear of background no additional washes were performed. If further washing was necessary, the blot was incubated twice for 20 minutes each at 65°C in high stringency wash prior to autoradiography. Autoradiography was carried out using Kodak X-Omat film in Fisher Scientific film cassettes with intensifying screens at -80°C.

Results

SSCP

PITX2 primers 2F/R to 9F/R were used to perform SSCP analysis on thirteen members of my study. SSCP results detected no alterations indicative of mutations or polymorphisms in any of the thirteen members of the study group for any primer pair used. Member DG from the ADA family was examined by SSCP after the mutation in DG had been detected (see below). The SSCP screen of DG was performed to confirm that the mutation detected in the PITX2 gene in this individual was the only mutation present in the PITX2 gene. The SSCP reactions were intended to provide a quick test for mutations in the PITX2 gene. However, since SSCP estimated to detect only 60-80% of mutations (Mirzayans, Walter, personal communication) and since the PITX2 gene is quite small, I sequenced the entire coding region of the PITX2 gene in all 14 ARS/IGDS patients to either confirm or refute the SSCP results.

Sequencing of the PITX2 Gene

ADA Family:

The ADA family is a large kindred with a disorder which has been linked by previous work to chromosome 4q25 (11, 46). ARS had previously been linked to 4q25. The PITX2 gene has recently been cloned from the same location (21). The ADA family presents with eye findings that are distinct from classical Axenfeld-Rieger syndrome and have been diagnosed as Iridogoniodysgenesis syndrome (IGDS) (11). Affected members of this family present with malformed angle of the anterior segment (goniodysgenesis), iris stromal hypoplasia and juvenile glaucoma, but not with iris adhesions or displaced Schwalbe's line characteristic of ARS (11, 46) (Table 1). Since the disorder in this family

with IGDS is linked to the same chromosomal location as families with ARS, the IGDS family was also included in the screening of the PITX2 gene for mutations. Mutational analysis of the PITX2 gene in the ADA family was initiated with published primers (21), shown in Table 3. PITX2 gene primers 4F/4R were initially used to amplify a portion of the PITX2 gene from a member of the ADA family presenting with IGDS. Initially the primer pair 4F/R produced a high quality single PCR product subsequently used in sequencing reactions. However, the primer pair 4F/R gave inconsistent results. Therefore, a new primer pair was designed: SK1/2 (Table 3, Figure 16). A "touchdown" PCR reaction using primers SK1 and 4R was performed, producing a single band of approximately 240 bp, the expected size of product for this primer pair. The SK1/4R primer pair spans the majority of the PITX2 homeodomain (Figure 16). Direct sequencing of the 4F/R PCR product from an individual affected with IGDS revealed a G to A transition (Figure 21). This is predicted to result in the conversion of an arginine to a histidine at the fourth amino acid residue in helix 2 of the homeodomain of PITX2 (Figure 21). Single strand conformation polymorphism (SSCP) analysis was carried out on the remaining affected and unaffected members of the IGDS family using primer pair SK1 and 4R (rather than the 4F/R primer pair as indicated above) to determine if this mutation segregated with the IGDS phenotype in this family. As indicated earlier, the initial SSCP scan of the PITX2 gene did not include this family. An extra band was observed in affected individuals which was absent in unaffected persons (Figure 22). One hundred chromosomes from the general population were also tested by SSCP. No extra bands, or any other alterations of the SK1/4R product, were observed in the control population. The predicted conversion of an arginine residue to histidine in helix 2 of the PITX2 homeobox occurs at a highly conserved residue and, therefore, may significantly affect PITX2 function (Figure 21 and Figure 26).

Figure 21. DNA sequence analysis indicating G to A missense mutation in the ADA family (23).

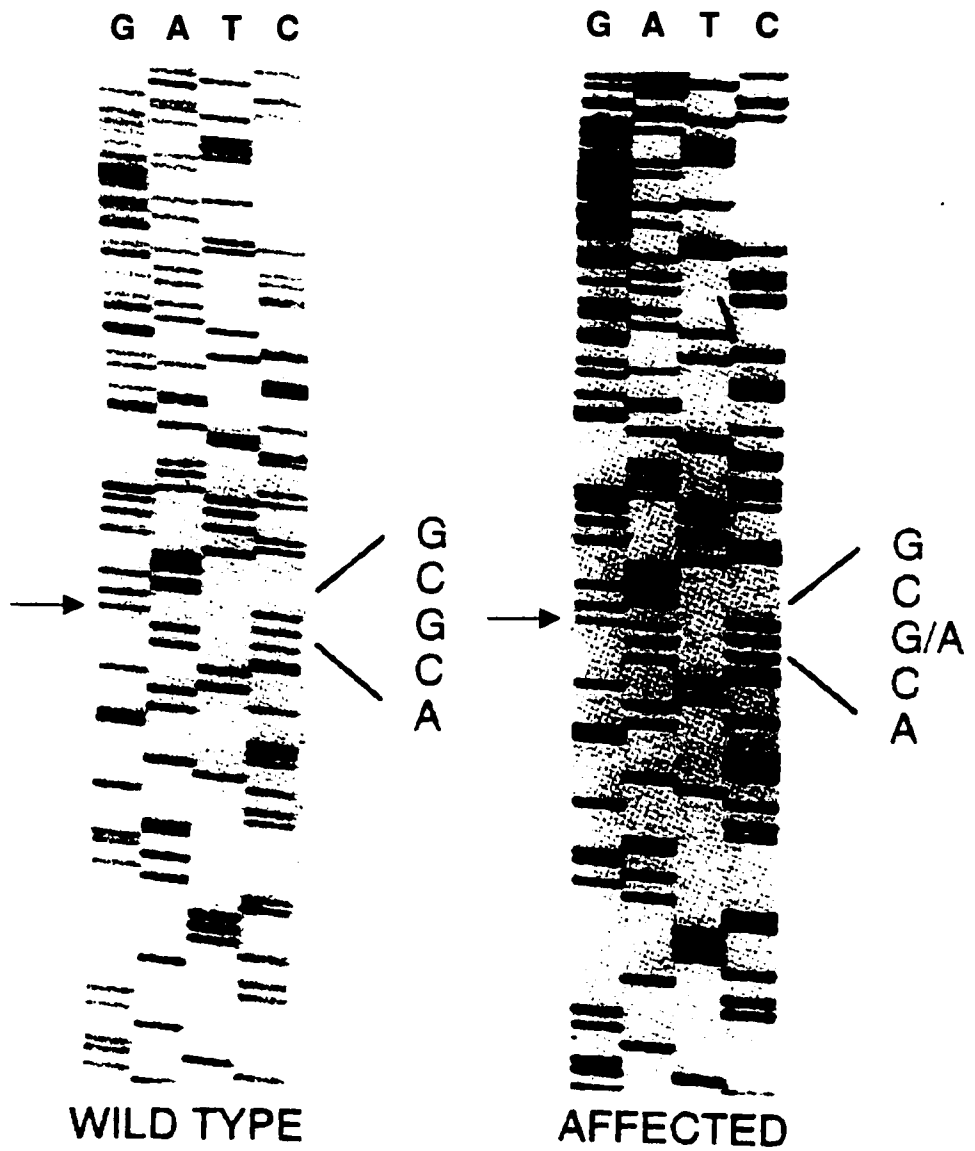
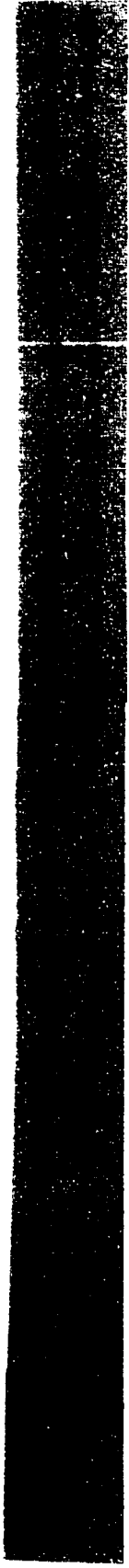
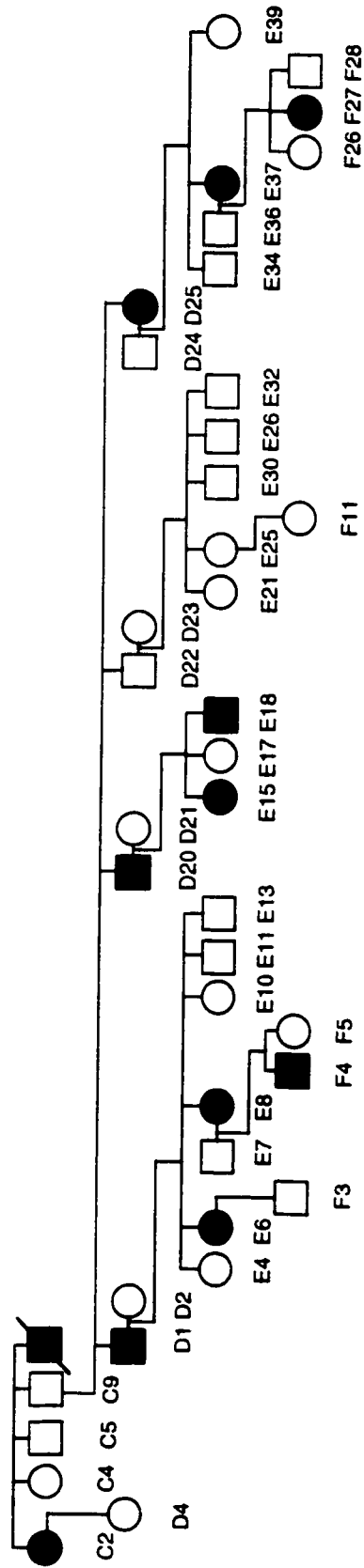


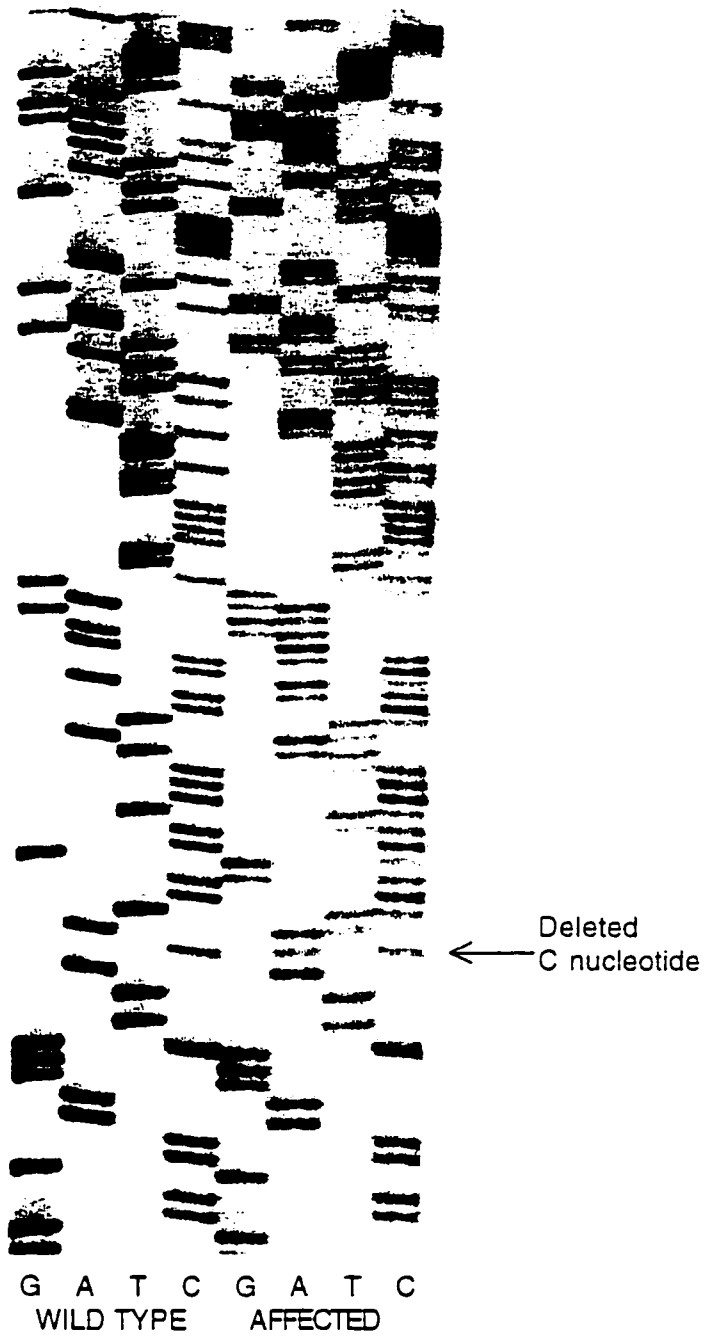
Figure 22. SSCP gel of ADA family indicating extra band present in affected individuals but absent in unaffected individuals.



RID Family

The RID family presents with a classical phenotype for Axenfeld-Rieger Syndrome (Table 2, individual KR). The ocular phenotype in the RID family includes iris hypoplasia, iris adhesions, displaced Schwalbe line, and non-ocular features characteristic of ARS including small, missing and misshapen teeth and a failure to involute of the periumbilical skin. Sequencing of the coding region spanned by primer pair 6F/R revealed a frameshift mutation (Figure 23). Specifically a deleted C residue at nucleotide 998 which results in an inframe premature stop codon fifteen amino acids downstream (Figure 23). This mutation was not detected by SSCP, and is not present in unaffected members of this family (results not shown). Although this mutation is not found in the homeodomain, it does result in the deletion of the conserved fourteen amino acids near the 3' end of the PITX2 coding sequence. It is possible that this conserved 14 amino acid downstream portion of PITX2 may be a key functional domain required for protein/protein interactions and therefore for proper PITX2 function (21).

Figure 23. Sequencing gel indicating frameshift mutation detected in the RID family. Position of deleted C nucleotide is indicated. The deletion is thought to result in a prematurely truncated PITX2 protein. The mutation was observed in affected family members but not in the unaffected family members.

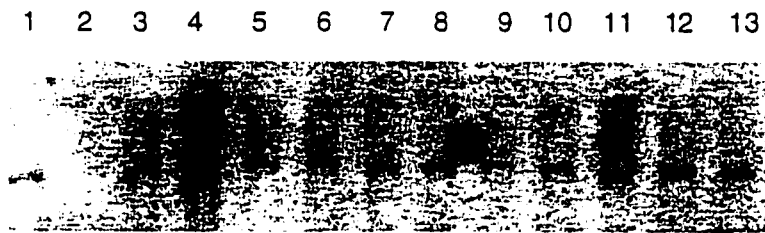


Southern Blot Analysis

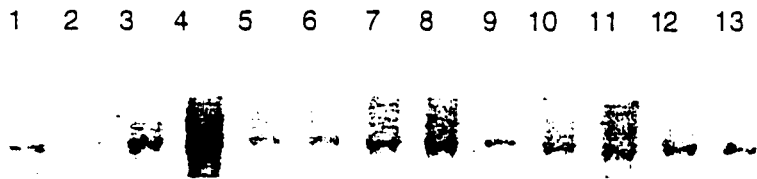
Recent work suggests that haploinsufficiency, either functionally or physically, of the PITX2 gene is the cause of ARS linked to 4q25 (47-53). Therefore, a deletion of the 4q25 region or translocation involving nearby regions which control PITX2 expression could also cause the ARS phenotype. No detectable chromosomal abnormalities of the 4q25 region were reported in the twelve persons in my study for which no mutation in PITX2 had been detected by DNA sequencing. Therefore, a Southern blot analysis was carried out on these 12 persons. As indicated in Methods and Materials, 3µg of total genomic DNA was digested with *EcoRI* and then transferred to Hybond-N membrane (Amersham Life Sciences) and probed with labeled PITX2 cDNA. FKHL7 was used as a control probe. The results of the Southern blot (Figure 24) show no obvious rearrangements of the DNA near the PITX2 or FKHL7 genes. Densitometry was used to examine the band intensities. Due to weak signals and high backgrounds, clear and consistent densitometry readings were difficult to obtain. Therefore the densitometry results were inconclusive as to whether or not a microdeletion had occurred in any of the affected persons indicated in Figure 24.

This experiment should be repeated in order to improve the quality of the signals or alternatively the technique of real time PCR could be employed to determine the copy number of the PITX2 genes present in the affected individuals in this study.

Figure 24. Genomic Southern probed with PITX2 cDNA and with FKHL7 cDNA. Approximately equal intensities observed in each individual with both probes (1=control, 2=CM, 3=JD, 4=MF, 5=LS, 6=AH, 7=AG, 8=KR, 9=MC, 10=DD, 11=MP, 12=GL, 13=BK).



Genomic Southern
Probed with PITX2 cDNA



Genomic Southern
Probed with FKHL7 cDNA

Marker Analysis

Three families (A, B, and C) were studied in a genetic marker screen (see Methods) to attempt to determine the linkage of the ARS phenotype segregating in these families for which no PITX2 mutation was detected (Figure 18, 19, 20). The following chromosomal regions were examined: 6p25, 11p13, 13q14 and 4q25. Loci at those regions known to be involved in eye development are FKHL7, PAX6, an unknown gene previously linked to one case of ARS (13), and PITX2 respectively.

Family A

Family A showed significant linkage to the chromosome 4 markers D4S2623 and D4S193. A final LOD score of 3.05 was calculated at a recombination frequency of 0.05 with marker D4S193 (Table 4). This suggests that a mutation undetected by the sequencing of the PITX2 gene or by Southern analysis is responsible for the phenotype presenting in family A. It is also possible, however that another as yet unidentified gene exists at the 4q25 chromosomal location that, when mutated, can also cause ARS. Clustering of genes involved in anterior segment disorders has previously been observed (35). Chromosomal region 6p25 has been shown to have at least two genes involved in eye development (35). Approximately 100 base pairs of the region upstream of the PITX2 transcription start site in family A was sequenced. The sequencing of the upstream region detected no mutations in family A. One other marker in the region of the PITX2 gene, D4S1651, was examined to assess linkage to 4q25 in this family. The results of this marker proved to be uninformative and no further markers were run on family A. Marker D4S2623 showed a peak LOD score of 3.00 at $\theta = 0.06$. Marker D4S193 showed a peak LOD score of 3.05 at $\theta = 0.05$. The markers D4S193 and D4S2623 are separated by approximately 3cM. The PITX2 gene is located between these two markers (www.Marshmed.org/genetics and 22, 52, 53).

Table 4 Linkage results for Family A

LOD Score at Recombination Fractions (θ)

Locus	0	0.02	0.05	0.1	0.2	0.3	0.4
D4S2623	$-\infty$	2.91	2.99	2.92	2.42	1.70	0.814
D4S193	1.64	2.98	3.05	2.95	2.40	1.64	0.739

Family B

All the chromosomal regions listed above were examined in family B (Figure 19) using polymorphic loci linked to these regions. LOD scores for these markers for family B ranged from approximately -3 to -12 indicating that none of these loci known to be involved in eye development are likely play a role in the ARS phenotype observed in this family (Table 5). D4S2623 showed a peak LOD score of -0.459 at $\theta = 0.4$. D11S907 showed a peak LOD score of -0.282 at $\theta = 0.4$. D13S263 showed a peak LOD score of 0.069 at $\theta = 0.4$. D6S344 showed a peak LOD score of -0.282 at $\theta = 0.4$

Table 5 Linkage results for Family B

LOD Score at Recombination Fractions (θ)

Locus	0	0.025	0.05	0.1	0.2	0.3	0.4
D4S2623	$-\infty$	-12.4	-6.88	-4.57	-2.37	-1.19	-0.459
D11S907	$-\infty$	-7.66	-5.60	-3.62	-1.76	-0.822	-0.282
D13S263	$-\infty$	-4.47	-3.05	-1.71	-0.56	-0.086	0.069
D6S344	$-\infty$	-7.66	-5.6	-3.62	-1.76	-0.822	-0.282

Family C

Negative LOD scores were obtained with markers for chromosome 13, 4 and 11 for family C (Figure 20 and Table 6). This effectively excludes the 13q14 locus linked to ARS by Phillips (13), the PITX2 gene at 4q25 and PAX6 at 11p13. D6S967, a polymorphic marker at 6p25, gave a peak LOD score of 1.47 at $\theta = 0.75$ (Table 6). This neither excludes nor confirms linkage to the region of 6p25 known to be associated with some cases of anterior segment disorders (35). At the moment, of this writing the markers utilized with Family C are not fully informative. If more markers and/or more affected family members' DNA becomes available, further studies with 6p25 markers may resolve the possible linkage of the phenotype observed in Family C to the 6p25 region. D6S967 showed a peak LOD score of 1.47 at $\theta = 0.075$. D13S1253 showed a peak LOD score of 0.101 at $\theta = 0.4$. D4S1651 showed a peak LOD score of -0.028 at $\theta = 0.4$. D4S2623 showed a peak LOD score of 0.574 at $\theta = 0.025$. D11S907 showed a peak LOD score of -0.071 at $\theta = 0.4$.

Table 6 Linkage results for Family C

LOD Score at Recombination Fractions (θ)

Locus	0	0.025	0.05	0.1	0.2	0.3	0.4
D4S1651	$-\infty$	-1.36	-0.899	-0.584	-0.276	-0.114	-0.028
D4S2623	0.602	0.574	0.574	0.478	0.331	0.176	0.049
D6S967	$-\infty$	1.24	1.42	1.46	1.21	0.783	0.327
D13S1253	$-\infty$	-0.55	-1.01	-0.469	-0.027	0.109	0.101
D11S907	$-\infty$	-4.89	-3.46	-2.10	-0.899	-0.339	-0.071

PAX6 Mutation in VA Family

The VA family, represented by individual AH, included in the study group did not fit the usual criteria for ARS (see Table 2). The VA family presented with nystagmus, corectopia, anterior stromal elliptical iris defects and optic nerve hypoplasia. No mutation in the PITX2 gene was detected in this family. However, since the phenotype in the VA family included optic nerve hypoplasia it was thought that PAX6 may be involved in the VA family phenotype since PAX6 has such a broad role in eye development including the developing optic nerve and embryonic fissure. An SSCP screen of the PAX6 gene was first carried out by Farideh Mirzayans to see if any shifts were visible. One shift was detected with primer pair 5F/R using standard SSCP techniques (see Methods). This PCR product was then sequenced. Sequencing revealed a frame shift mutation (a one bp deletion) in exon 5 of PAX6 predicted to result in premature truncation of the PAX6 protein 15 amino acids downstream. The truncated protein is missing approximately 75% of the downstream portion of the paired box and all the subsequent downstream portions of the gene, including the functional homeobox in the 3' region (Mirzayans, personal communication).

Discussion

PITX2 missense mutation in a family with IGDS

Direct sequencing and SSCP analysis have demonstrated that an individual in the ADA family, diagnosed with IGDS, had a G to A missense mutation in the fourth amino acid in helix 2 of the homeodomain of the PITX2 gene. This coding sequence alteration is predicted to result in a change from the wildtype sequence of CGC (Arg 70) (23) to CAC (His70) (Figure 25). A comparison of the PITX2 sequence with 346 known homeobox sequences reveals that this residue of helix 2 is an arginine (Arg) in 81% of homeotic genes but has never been observed to be a histidine (His) (54). This amino acid position is an arginine in all bicoid class homeotic genes (21)(Figure 26). The helix-turn-helix pattern seen in PITX2 conforms to the classic homeodomain DNA binding motif (54, 55). The downstream helix (Helix 3) is thought to fit into the major groove of DNA and establish contact with specific residues (54, 55). The upstream helix (Helix 2) is then thought to come into position in such a way as to make contact with phosphate residues in the backbone of DNA and stabilize the interaction of helix 3 with the DNA residues in the major groove (54, 55, 56). The Arg residue mutated in the IGDS family is one of the contact points between the DNA phosphate backbone and helix 2 of homeodomain proteins (54, 55, 56). These findings suggest that the mutation of Arg70 to a His70 in this critical region of the homeodomain of PITX2 could destabilize the interaction of the PITX2 protein with the target sequences of the gene(s) with which it interacts.

The discovery of a mutation in PITX2 in a family with IGDS also demonstrates that IGDS and ARS are allelic disorders. PITX2 mutations were previously identified in patients with ARS (21). Both ARS and IGDS are characterized by ocular findings that include iris hypoplasia and increased intra-ocular pressure (38). Both ARS and IGDS also

Figure 25. Figure showing amino acid sequence of several members of the bicoid class of homeobox genes. Asterisk indicates location of arginine residue predicted to be converted to a histidine residue in the ADA family. Rieg1 and Ptx1 are the mouse homologues of PITX2 and PTX1 respectively. Unc-30 is the PITX2 homologue in *C. elegans*. Otx genes are involved in formation of the anterior structures of the vertebrate head including the eye.

%identity
with RIEG1

helix 1 helix 2 helix 3/4

Consensus QRRQRTHFTS .QL.ELEA.F .RNRYPDM.. REEIAVW.NL TE.RVRVWFK NRRAKWRKRE

RIEG1 Q..Q...T. Q.....ST T... A.....

Riegl Q..Q...T. Q.....ST T... A.....

Ptx1 Q..Q...T. Q.....SM T... P.....

UNC-30 H..T...NW. S.....AC IS. P.....

OTX1 .E..T..R S..DV...L. AKT.....IFM .V.LKI.. P.S..Q.....O.QQQ

OTX2 .E..T..R A..DV...L. AKT.....IFM .V.LKI.. P.S..Q.....O.QQQ

100
97
83
62
62

present with non-ocular features including maxillary hypoplasia, missing and misshapen teeth and a failure of involution of the periumbilical skin (38). However, patients with ARS also present with a prominent Schwalbe line and adhesions between the cornea and iris which are not present in IGDS patients (38). Since ARS and IGDS can result from mutations in the same gene, each disorder can be seen as existing along a spectrum of severity with the same underlying cause. It is tempting to speculate that the missense mutation (Arg70His) found in this IGDS family could result in residual function of the PITX2 gene that could in turn lead to a milder eye phenotype than ARS. However, the considerable phenotypic variation observed within ARS families could preclude a straightforward genotype/phenotype correlation (57).

Another example of IGDS being caused by mutations in the PITX2 gene has been reported by Alward et al. (58). A mutation in the PITX2 gene was found in an individual presenting with autosomal dominant iris hypoplasia. The autosomal dominant iris hypoplasia observed in the individual in which the mutation was detected is similar in phenotype to IGDS. The iris stromal layer is very thin such that the underlying pigment layer of the iris and pupillary sphincter muscle are visible (10). The mutation detected was also shown to segregate with the phenotype in the family involved in the study and is therefore, thought to cause the observed eye disorder (58). One individual related to the proband also presented with dental anomalies. A C to T nucleotide conversion at arginine 46 (the 136th nucleotide residue) in the PITX2 homeobox was detected. This mutation is predicted to result in the conversion of an arginine residue to a tryptophan residue. Alward et al. speculate that this non-conservative R46Y mutation could result in either altered protein structure or function (58).

The discovery that mutations in PITX2 can cause two clinically distinct eye disorders, ARS and IGDS, is consistent with the phenotypic variability observed with PAX6. Mutations in PAX6 have been shown to cause a range of eye malformations

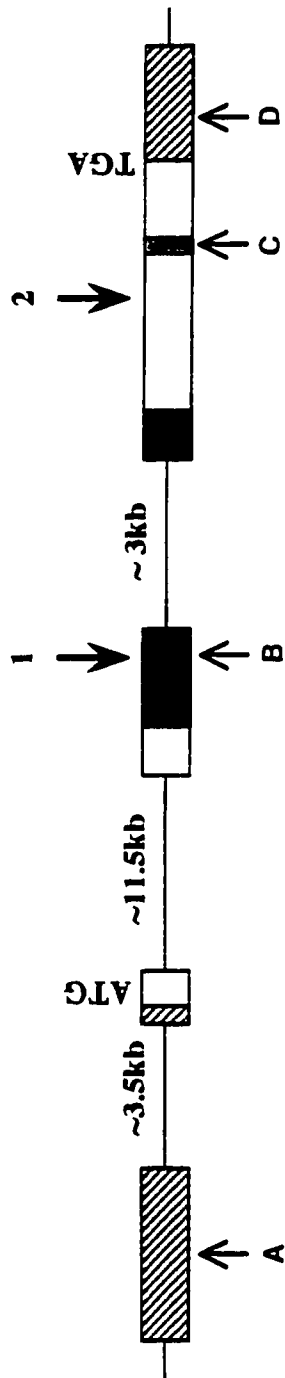
including aniridia, autosomal dominant keratitis, and Peter's anomaly and anterior segment disorders (28, 30, 31, 60).

Mutations of the PITX2 gene have a substantial effect upon development of the eye, teeth and jaw suggesting that PITX2 plays a key role in human craniofacial development. The current finding that IGDS and ARS both can result from PITX2 mutations implicates PITX2 broadly in ocular and craniofacial disorders.

PITX2 frameshift mutation in a family with classical ARS

A frameshift mutation in the PITX2 gene was discovered in the RID family (represented by individual 'KR'. Table 2). The RID family presents with a classical ARS phenotype including iris hypoplasia, iris adhesions, displaced Schwalbe line, and non-ocular features characteristic of ARS including small, missing and misshapen teeth and a failure to involute of the periumbilical skin (Table 2). The frameshift is caused by a deleted cytosine residue at nucleotide 998 in the PITX2 coding sequence (Figure 23). The mutation occurs downstream of the homeobox and is predicted to create an in frame TGA stop codon fifteen amino acids downstream of the deleted residue. The location of the mutation is such that the homeobox remains intact but most of the 3' coding sequence of the gene is deleted (Figure 26). This mutation is predicted to result in the truncation of the PITX2 protein including a stretch of 14 amino acids which have been suggested to be highly conserved in bicoid class transcription factors (21). Although the exact function of this conserved stretch of amino acids has not yet been determined, Semina et. al. have postulated that these amino acids may be needed for protein/protein interactions (21). These protein/protein interactions could be part of the mechanism which directs normal PITX2 function. When these fourteen amino acids are missing the normal spatial and/or temporal functioning of PITX2 or proteins it interacts with may be disturbed. It is also possible that the downstream portions of the PITX2 gene missing in this mutation are

Figure 26. Diagram showing location of two mutations in PITX2 gene detected by my research. 1= missense mutation (G to A) detected in the ADA family. 2= the deleted C nucleotide seen in the RID family. A = 3' UTR, B = Homeo Box (note that the Homeo Box is split by intron 3), C = conserved 14 amino acid stretch, D = 5' UTR.



needed for the normal structure of the protein and, when missing, the protein is destabilized in some way that prevents its normal function.

Genotype Phenotype Correlations in PITX2 Mutations

The two families in which I detected PITX2 mutations indicate that it may be possible to draw genotype/phenotype correlations in regards to mutations in the PITX2 gene.

The RID family, which presents with classical ARS, is carrying a PITX2 mutation which is predicted to cause a drastic alteration in protein structure by eliminating a large portion of the gene's coding sequence, including a stretch of conserved amino acids. This conserved stretch of amino acids may play a key role in the functioning of the PITX2 gene product either with its target DNA sequences or with other proteins. In this way, the frameshift mutation seen in the RID family may cause a dramatic change in PITX2 gene function.

The ADA family presents with a much more subtle mutation. In this family, the disease causing mutation is a missense mutation at a key residue in the second helix of the homeobox of the PITX2 gene (Figure 26). As described above, this mutation is thought to alter a key amino acid residue which functions in stabilizing the interaction of the PITX2 protein with its target DNA sequence. The ADA family also presents with a much milder eye phenotype than the RID family. The ADA family presents with iris hypoplasia as does the RID family but the ADA family does not have iris adhesions to the cornea or a displaced Schwalbe line, indicating that the eye has developed more normally in the ADA family than in the RID family. In Semina's paper discussing the cloning of the PITX2 gene, the ARS patients involved in the study all presented with the classic signs of ARS (Table 1)(21). The mutations described by Semina and colleagues include two non-conservative amino acid substitutions in the PITX2 homeodomain

predicted to substantially disrupt the structure of the homeodomain, two possible splice site mutations with undetermined results to the PITX2 coding structure and a nonsense mutation predicted to result in a premature stop codon located between the homeobox and the conserved 14 amino acid domain (described previously). When taken together, the mutations detected by Semina (21), Alward (58) and by my research seem to support the conclusion that severe disruption of the structure or function of the PITX2 gene can be correlated with a more severe eye phenotype (described as ARS). A less disruptive mutation seems to be associated with fewer disturbances in eye development (classified as IGDS).

Frequency of ARS cases caused by PITX2 Mutations

It is interesting to note that in our particular cohort of ARS/IGDS patients only two mutations were detected in the PITX2 gene. This is a frequency of only 14%. The original paper, which describes the cloning of the PITX2 gene, Semina and colleagues reported that a mutation frequency of 30% was seen in the PITX2 gene in patients with ARS symptoms (21). Both of these data sets indicate that between 70 and 85% of ARS cases may result from mutations in genes other than PITX2.

The scarcity of mutations raises some interesting questions as to what other genes are responsible for the Axenfeld-Rieger phenotype or what mutations may have been missed in the PITX2 gene: e.g. promoter and regulatory mutations or mutations in genes responsible for proper PITX2 function. Further linkage studies in families with anterior segment malformations may lead to the identification of other genes involved in human craniofacial development.

Overall, the sequencing of the PITX2 gene has shown a low percentage of mutations in families diagnosed with ARS or IGDS (Table 2). Of fourteen families in the

cohort two mutations have been detected by direct sequencing of the PITX2 gene coding region.

Genes other than PITX2 Causing ARS

A second ARS locus has been mapped to 13q14 by Phillips and coworkers (13). The family used in the study presented with sensorineural hearing loss in addition to the standard features of ARS (13). Therefore, it is possible that patients with ARS caused by mutations in a gene at 13q14 could be distinguished on the basis of the additional phenotypic finding of sensory hearing loss. None of the patients in my study presented with any type of hearing loss and, therefore, it is unlikely that mutations in the gene at 13q14 are causative of the ARS phenotype in any family in my cohort. Even though none of the three families was large enough to conduct linkage analysis on, linkage to 13q14 was investigated. Other candidate genes involved in eye disease exist in the genome and several of them were also examined for linkage in the same three families. The other regions/genes examined for linkage were PAX6 (11p13), FKHL7 (6p25) and PITX2 (4q25). The PITX2 gene region was also checked for linkage in order to ascertain if a mutation may have been missed despite the complete sequencing of the known PITX2 coding regions.

Family A showed what may be the most interesting linkage result. The disorder in this family was shown to have significant linkage disequilibrium to marker D4S2623 (Table 4). This result indicates that Family A is linked to the PITX2 region of chromosome 4. However, no mutation in the PITX2 was detected in Family A. This raises several possibilities. First, that Family A has have a mutation that was not detected in the PITX2 gene. This seems unlikely as the sequencing results were of high quality and sequencing autoradiographs were analyzed in triplicate. Key regions of the gene (eg.

the homeobox) were sequenced twice to make sure that there were no mutations present. Primer pair 1F/R (see methods) was used to amplify a stretch of the upstream region of the PITX2 gene in this family. No mutation was observed in the upstream portion of the gene near the start site.

A further possibility to explain the linkage of Family A to 4q25 is that the PITX2 gene may undergo alternative splicing events. At least one alternately spliced exon is known to exist in PITX2 (40). This exon has been examined in all the individuals in my study but it has been suggested that PITX2 may have several naturally occurring isoforms (21). It may be possible that the mutation in Family A is located in the coding sequence of one or more of these other forms and therefore was not detected from the sequencing of the PITX2 coding sequence as it is understood at this time. In addition the possibility exists of a mutation present inside an intron which could cause the activation of a cryptic splice site. This could result in a greatly modified PITX2 protein with altered or absent function.

Finding no mutation in the family with ARS linked to 4q25 raises the possibility that there is another gene in the same region as PITX2 which could cause ARS. A precedent for this possibility has been shown to exist at 6p25. It has now been shown that two or more genes relevant to eye formation exist at the tip of the short arm of chromosome 6 (35). One gene, FKHL7, has now been shown to be mutated in persons with ARA (35, 36). However, several families are known in which critical recombination events rule out FKHL7 as the only eye development gene in that region (35). Perhaps the situation is similar on 4q25 and other genes, which have not yet been discovered, are involved in the formation of the eye. Recent work has also detected a mutation in the FKHL7 gene in a family with ARS (Mirzayans et. al. In press). This discovery indicates that mutations in FKHL7 are responsible for both ARA/ARS while the PITX2 gene has only been implicated in ARS/IGDS. Why FKHL7 is involved in both the syndromic and

non-syndromic versions of these eye diseases and PITX2 is involved only in the syndromic forms should be elucidated by further investigation.

Murray and coworkers have recently discovered mutations in the PITX3 gene in patients with anterior segment mesenchymal dysgenesis (ASMD) indicating that there are certainly other genes involved in the same developmental pathway as PITX2 affecting the anterior segment of the eye (60). The PITX3 gene is located on chromosome 10q25 in the human and 19 in the mouse. PITX3 appears to be mostly involved in proper lens development. ASMD is an eye disorder characterized by corneal opacities, which can occur with or without iris adhesions, cataracts, and occasionally optic nerve abnormalities (60). These characteristics have some similarity to characteristics seen in ARS and IGDS. Linkage analysis on families affected with anterior segment disorders may provide some clues as to whether or not PITX3 may be involved in the ARS/IGDS type of disorder.

Marker Summary

Of the three families on which linkage analysis was carried out, one family showed linkage to the region of the PITX2 gene at 4q25 (Table 4). As discussed previously, the coding sequence and some promoter sequence of this family was shown to be free of mutations raising the question of what is responsible for the phenotype seen in this family. The PITX2 gene could contain some unknown coding sequence, or perhaps there is another gene present in the 4q25 region related to eye development.

The linkage results for the other two families indicate that the gene(s) responsible for the observed phenotype are not linked to any of the known candidate gene(s) or loci in these families (Tables 5 and 6). The genes, PITX2 and PAX6, and loci at 13q14 and 6p25, have all been shown to be unlinked to the phenotype seen in families B and C. This indicates that other undiscovered loci related to eye development are likely to be mutated in these two families.

Vertebrate development

The development of a multicellular organism is a complex series of events directed by the genetic information contained in that organism. The PITX2 gene has been shown to be one of the genes involved in vertebrate development, specifically in the development of the vertebrate craniofacial structures. Recent work has shown that PITX2 is also involved in the proper formation of structures other than the vertebrate eye and head.

PITX2 Involvement in Vertebrate Body Plan Development

The development of the vertebrate body plan is the result of a series of complex genetic and biochemical events. An interesting feature of the vertebrate body plan is that although symmetrical on the left/right axis on the exterior, the interior of the body shows marked asymmetry. Many of the genes involved in the development of the vertebrate body plan have been elucidated and include nodal, sonic hedgehog, lefty 1 and 2, activin and cSnR (61-68). These genes show distinct left/right variations in expression that implicates them in the formation of the internal asymmetry seen in vertebrates. Two recent papers published in Cell (69, 70) have implicated PITX2 in the normal left/right asymmetry seen in the vertebrate body plan. Expression studies in the mouse show bilateral PITX2 expression as early as stage 6 bilaterally in the head mesenchyme, as would be expected of a gene known to be involved in eye formation. However, PITX2 expression at later stages of development in the mouse has been shown to be asymmetrical (69, 70). At stage 7, PITX2 expression is seen in the left side of the lateral plate mesoderm and by stage 10, PITX2 expression is observed in the left presumptive myocardium (69, 70). By stage 15, PITX2 expression continues bilaterally in the mandible, maxilla and periocular mesenchyme, which is consistent with PITX2 being

involved in craniofacial development. Also, at stage 15, PITX2 expression continues to be asymmetrically expressed in the left side of the developing heart and gut, reinforcing the conclusion that PITX2 is part of the molecular pathway determining left/right asymmetry in vertebrates (69, 70).

This recent work on the involvement of PITX2 in the development of vertebrate systems other than the eye, illustrates that PITX2 is one of the key genes in overall vertebrate development. Further study of the activity of the PITX2 gene product may elucidate its role in other developmental anomalies and increase our understanding of some of the complex steps in human development.

PITX2 and interactions with target DNA sites and other proteins

Once a gene has been cloned, determining its biological function and mode of action can prove to be just as challenging as the efforts to clone the gene. Now that the PITX2 gene has been identified, it is necessary to determine its biological role in development. Since PITX2 is a transcription factor, it is likely to bind to DNA and effect the expression of other genes. It is also quite likely that in order to perform biological functions, the PITX2 gene product may interact with other proteins, possibly including other transcription factors. Amend and co-workers in 1998 (71) took some initial steps in determining the biological activity of the Pitx2 gene product. Amend's work showed that the Pitx2 product binds to the bicoid consensus sequence of 5'-TAATCC-3' (71). This is consistent with Pitx2 being a member of the bicoid family of transcription factors as shown by the presence of a lysine residue at position 50 of the homeobox in Pitx2 (21). Further to this Amend et. al demonstrated that the Pitx2 product was also able to bind with the Pit1 gene product in vitro. This protein/protein binding produced an increase in PITX2 binding and transcriptional activity as indicated by the expression of a reporter gene downstream of the bicoid binding sequence (71).

In Semina and colleagues' original paper on the cloning of the PITX2 gene, several mutations were identified that segregated with the disorder and were therefore thought to be causative of ARS (21). In the paper on the biological activity of the Pitx2, Amend examined the function of two of the mutations discovered by Semina (71). The two mutations examined were a threonine to proline conversion at amino acid residue 68 (T68P) and a leucine to glutamine conversion at amino acid residue 54 (L54Q) (21, 71). The T68P mutation observed by Semina produced a noticeable drop in the binding specificity of Pitx2. This was indicated by the ability of the mutant to bind DNA sequences other than the bicoid consensus although the ability to bind to DNA was still present (71). Also the ability of Pitx2 to activate transcription of reporter genes was no longer present (71). Further to this, the T68P mutation in Pitx2 still allowed for the binding of Pitx2 to Pit1 but this mutation did eliminate the synergistic activity of these two transcription factors on the expression of the prolactin gene (71). Pitx2 has also been observed to transcriptionally activate the prolactin gene without binding to Pit1. However the prolactin transcribing activity of Pitx2 is no longer observed in the T68P mutant (71). The prolactin gene is expressed in certain cellular subtypes of the anterior pituitary and is thought to be necessary for the normal differentiation of this endocrine gland (72, 73, 74). Pit1 is a POU domain transcription factor known to activate expression of the prolactin gene during development (72, 73, 74). Pit1 also binds to the Pitx2 related protein Pitx1 (72, 73, 74).

The L54Q mutation produced a Pitx2 protein thought to be structurally unstable as no activity or product was observed in any experiments (71). The location of the suspected amino acid conversion of a leucine to a glutamine occurs at a highly conserved residue in the Pitx2 coding region, which is suspected of playing a key role in the normal function and/or structure of Pitx2 (71).

It would be interesting to see if the phenotypes of these two different cases of Axenfeld-Rieger syndrome is noticeably different. However, no mention of any

phenotypic variation in individual patients that would relate genotype with phenotype was described by the authors. In my work, I have observed that a milder disruption in the coding sequences of the PITX2 gene results in a less severe eye phenotype as seen in the ADA family and that a more severe disruption of the PITX2 gene results in a more severe phenotype as observed in the RID family (see above). The work by Amend and co-workers indicates that the two different mutations studied result in drastically different Pitx2 activities. The T68P mutation results in some residual activity, while the L54Q mutation abolishes Pitx2 activity. These two mutations may also result in different eye phenotypes due to the varying levels of residual Pitx2 activity.

Investigations are also underway to investigate the affects on PITX2 function caused by the mutations I isolated in the course of my graduate research. The effect of the ADA family missense mutation in the PITX2 homeobox upon binding of DNA by PITX2 is being studied.

Haploinsufficiency as a Cause of Axenfeld-Rieger syndrome

Axenfeld-Rieger syndrome is an autosomal dominant disorder. When one copy of the PITX2 gene is mutated then the disorder will occur. This information does not, however, tell us whether the mutant copy of the gene interferes with the function of the remaining copy (the dominant-negative effect) or whether the loss of function of one copy of the gene results in insufficient normal gene product being produced to provide for normal function (haploinsufficiency). Numerous studies indicate that ARS results from haploinsufficiency of the PITX2 gene (47-53).

One patient in the study by Flomen had a deletion of chromosomal bands 4q25 to 4q27 (46, XX, del(4) (pter-q23::q27-qter) (48, 51). This region contains the PITX2 gene responsible for some cases of ARS (21). The other patient in the same study by Flomen

has a balanced translocation involving 4q25 and 12q15 in which the breakpoint of the translocation was determined to be 90kb away from the PITX2 coding region (46,XX, t(4;12)(q25;q15) (48, 75). These two chromosomal aberrations and the resulting phenotypes indicate that loss of one copy, either by deletion or by loss of function, of the PITX2 gene product, is capable of causing Axenfeld-Rieger Syndrome (48).

Studies by Murray and co-workers during the initial steps toward cloning the ARS gene also showed that haploinsufficiency of the PITX2 gene product is sufficient to cause ARS (52, 53). In the two translocation cases studied by Murray's group, the chromosomal breakpoints involved regions proximal to 4q25: 46,XX, t(4;11)(q27;q21) and 46, XX, t(4;16)(q26;q22). This finding supported the conclusion that the 4q25 region is crucial in the development of ARS. The finding that the 4q25 chromosomal breakpoints in both of these ARS cases fall outside the PITX2 gene is suggestive of the presence of cis-acting regulatory elements in the q25 band of chromosome 4 that are necessary for the normal expression of the PITX2 gene (52, 53). A translocation breakpoint near to the PITX2 gene would result in the functional, not physical, elimination of the PITX2 gene and haploinsufficiency of the PITX2 gene product would result in Axenfeld-Rieger syndrome (52, 53).

Schinzel described the case of a boy with ARS (47). The father of the child carried a interstitial translocation of bands 4q25-27 from chromosome 4 to chromosome 6 (46, XY, ins (6;4)(q26;q24q26)). The child inherited the derivative chromosome 4, lacking the 4q25-27 segment and thus lacking the PITX2 gene, from his father while the child received a normal chromosome 4 from his mother. The genotype of the child is thus 46, XY, del (4)(q24q26). This situation resulted in the child having only the maternal copy of the PITX2 gene (47). Despite having an interstitial translocation of 4q25-26 the father shows no features of ARS. Since no cases of non-penetrance for ARS have been reported, it can be concluded that the father has two normal copies of the PITX2 gene and

that the translocation breakpoints in the father do not disrupt the PITX2 gene. The child's ARS thus results from the haploinsufficiency of the PITX2 gene.

One other possible conclusion to the work of Flomen (75), Schinzel (47) and Murray (22) is that there is another gene in the 4q25 region which is also involved in eye development. This would be consistent with the fact that Family A studied in the linkage experiments demonstrates significant linkage to polymorphic markers in the 4q25 region and yet shows no mutation in the PITX2 gene (see results). Recent work by Mears and colleagues has also demonstrated that more than one gene involved in eye development is likely to reside in the 6p25 chromosomal region (16). Perhaps the 4q25 region also contains more than one gene involved in eye development.

Mechanisms of the ARS disorder

In 1983, Shields speculated on the mechanism of formation of the anterior segment disorder in Axenfeld-Rieger syndrome (ARS) may occur (76). Shields studied a group of 24 patients over a seven year time span. These patients were all diagnosed with either Axenfeld or Rieger anomaly/syndrome (76). Detailed analysis of the anterior segment of the individuals studied by Shields was performed in order to accurately determine the phenotype of each individual.

Shields reached several conclusions as a result of the study. Firstly, that Axenfeld and Rieger anomalies/syndromes are variations of the same disorder. Also, Shields concludes that ARS is a separate disorder from Peter anomaly and from Iridocorneal Endothelial syndrome (ICE). Peter Anomaly is a severe malformation in anterior segment formation characterized by central corneal opacifications, adhesions between the lens and/or iris and posterior surface of the cornea, and iris hypoplasia (60). Mutations in the PAX6 gene have been detected in some cases of Peter Anomaly (60). ICE is an anterior segment disorder which also frequently presents with secondary glaucoma (76). It is

distinct from ARS in that ICE seems to be a malfunction resulting from abnormal proliferation of the corneal endothelium (76). The phenotype observed in ARS is thought to result from a developmental arrest late in gestation by cells of neural crest origin (76). During development, the anterior chamber of the eye, the pupil is covered with a membrane referred to as the pupillary membrane. As the development of the eye progresses, this membrane normally disappears and is completely gone by birth. In the ARS phenotype, it is thought that this embryonic membrane persists. Remnants of the membrane, present on the iris and near Schwalbe's line, are thought to result in the strands of tissue often observed between the anterior surface of the iris to the cornea. In ARS contraction of this membrane is also thought to produce the abnormalities often observed in the pupil. Abnormal vasculature in and around the anterior segment is often observed in ARS patients as well. Shields postulated that abnormal vascularization may be causative of the iris hypoplasia observed in ARS. Shields described how the cells near Schwalbe's line showed altered collagen structures which may be related to the persistent membrane, as well as physical characteristics of the tissues present in the angle of the eye (76). Shields observed that patients with ARS displayed maldevelopment of the trabecular meshwork and Schlemm's canal. The inter-cellular spaces in the trabecular meshwork of a patient with ARS were smaller or missing. Schlemm's canal was absent or greatly diminished in size (76). Shields concluded that the glaucoma observed in approximately one-half of ARS patients resulted from the malformed trabecular meshwork and Schlemm's canal. The iris root has often been observed inserted in an anterior position covering some of the trabecular meshwork in ARS patients. This aberrant positioning of the iris may also contribute to the reduction in outflow of aqueous humor and consequently elevated intraocular pressures by compacting Schlemm's canal and the inter-cellular spaces of the trabecular meshwork (76).

From this study, Shields concluded that ARS results from a developmental arrest in the formation of the anterior segment of the eye. This arrest could result from some

disturbance in formation or regression of blood vessels such that tissue persists that should be absent from the anterior segment of the eye. This persistent tissue results in the observed phenotype, and explains the increased risk for developing glaucoma observed in ARS patients (76).

Conclusions

Axenfeld-Rieger syndrome was first described as a genetic disorder over 80 years ago (5, 6). PITX2, one of the genes responsible for this disorder has only recently been cloned and subjected to molecular biological studies (23, 21, 58). Recent evidence indicates that the PITX2 gene is indeed a key component of both eye and body development in vertebrates. However, the low frequency of PITX2 mutations observed in cases of ARS indicates that many cases of malformations of the anterior segment of the eye are likely to be caused by genes other than PITX2. Further studies on the function of PITX2 and isolation of other genes involved in eye development should lead to a greater understanding of human eye and craniofacial development and possibly vertebrate body plan formation. Continued studies should also help increase our understanding of the etiology and treatment of glaucoma by elucidating the mechanisms and physiology of pressure regulation in the eye.

References

1. Barishak, Y. R. 1992. Embryology of the eye and its adnexae. Developments in Ophthalmology. W. Straub, editor. Karger press.
2. Mann, I. 1964. The development of the human eye. Grune & Stratton, Inc., New York.
3. Shields, M., Bruce. 1998. Textbook of Glaucoma. Williams and Wilkins,
4. Liu, C., Heon. 1997. Genetics of Glaucoma: an update. *Can. J. Ophthalmol.* 32:221-228.
5. Axenfeld, T. 1920. Embryotoxon corneae posterius. *Ber Deutsch Ophthalmol Ges.* 42:381-382.
6. Rieger. H. 1934. Verlagerung und Schitzform der Pupille mit Hypoplasie des Irisvordblattes. *Z. Augenheilk.* 84:98-99.
7. Rieger, H. 1935. Beitrage zur Kenntnis seltener Missbildungen der Iris: Uber Hypoplasie des Irisvorderblattes mit Verlagerung und Entrundung der Pupille. . *Albrecht von Graefes Arch. Klin. Exp. Ophthalm.* 133:602-635.
8. Rieger, H. 1941. Erbfragen in der Augenheilkunde. . *Albrecht von Graefes Arch. Klin. Exp. Ophthalm.* 143:277-299.
9. Fitch, N. and M. Kaback. 1978. The Axenfeld syndrome and the Rieger syndrome. *Am. J. Med. Genet.* 15:30-34.
10. Héon, E., B. P. Sheth, J. W. Kalenak, S. L. Sunden, L. M. Streb, C. M. Taylor, L. M. Alward, V. C. Sheffield and E. M. Stone. 1995. Linkage of Autosomal dominant iris hypoplasia to the region of the Rieger syndrome locus (4q25). *Hum Mol Genet.* 4:1425-1439.
11. Walter, M. A., F. Mirzayans, A. J. Mears, K. Hickey and W. G. Pearce. 1996. Autosomal-dominant iridogoniodysgenesis and Axenfeld-Rieger syndrome are genetically distinct. *Ophthalmology.* 103:1907-15.

12. Berg, F. 1932. Erbliches jugendliches Glaukom. *Acta Ophthalmol.* 10:568-587.
13. Phillips, J. C., E. A. Del Bono, J. L. Haines, A. M. Pralea, J. S. Cohen, L. J. Greff and J. L. Wiggs. 1996. A second locus for Rieger syndrome maps to chromosome 13q14. *Am J Hum Genet.* 59:613-619.
14. Jerndal, T. 1972. Dominant goniodysgenesis with late congenital glaucoma: a re-examination of Berg's pedigree. *Am J Ophthalmol.* 74:28-33.
15. Weatherill, J. R. and C. T. Hart. 1969. Familial hypoplasia of the iris stroma associated with glaucoma. *Br J Ophthalmol.* 53:433-438.
16. Mears, A. J., F. Mirzayans, D. B. Gould, W. G. Pearce and M. A. Walter. 1996. Autosomal dominant iridogoniodysgenesis anomaly maps to 6p25. *Am J Hum Genet.* 59:1321-7.
17. Freund, C., D. J. Horsford and R. R. McInnes. 1996. Transcription factor genes and the developing eye: a genetic perspective. [Review] [234 refs]. *Hum Mol Genet.* 5:1471-1488.
18. Sarfarazi, M. 1997. Recent Advances in Molecular Genetics of Glaucomas. *Hum Mol Genet.* 6:1667-1677.
19. Kumar, J. and K. Moses. 1997. Transcription factors in eye development: a gorgeous mosaic? [comment]. [Review] [47 refs]. *Genes & Development.* 11:2023-8.
20. Graw, J. 1996. Genetic aspects of embryonic eye development in vertebrates. [Review] [146 refs]. *Developmental Genetics.* 18:181-97.
21. Semina, E. V., R. Reiter, N. J. Leysens, W. L. Alward, K. W. Small, N. A. Datson, B. J. Siegel, N. D. Bierke, P. Bitoun, B. U. Zabel, J. C. Carey and J. C. Murray. 1996. Cloning and characterization of a novel bicoid-related homeobox transcription factor gene, RIEG, involved in Rieger syndrome. *Nat Genet.* 14:392-9.
22. Murray, J. C., S. R. Bennett, A. E. Kwitek, K. W. Small, A. Schinzel, W. L. Alward, J. L. Weber, G. I. Bell and K. H. Buetow. 1992. Linkage of Rieger syndrome to the region of the epidermal growth factor gene on chromosome 4. *Nat Genet.* 2:46-9.

23. Kulak, S. C., K. Kozłowski, E. V. Semina, W. G. Pearce and M. A. Walter. 1998. Mutation in the RIEG1 gene in patients with iridogoniodysgenesis syndrome. *Hum Mol Genet.* 7:1113-1117.
24. Gruss, P. and C. Walther. 1992. Pax in development. *Cell.* 69:719-22.
25. Walther, C., J. L. Guenet, D. Simon, U. Deutsch, B. Jostes, M. D. Goulding, D. Plachov, R. Balling and P. Gruss. 1991. Pax: a murine multigene family of paired box-containing genes. *Genomics.* 11:424-34.
26. Strachan, T. and A. P. Read. 1994. PAX genes. *Curr Opin Genet Devel.* 4:427-438.
27. Eccles, M. R., L. J. Wallis, A. E. Fidler, N. K. Spurr, P. J. Goodfellow and A. E. Reeve. 1992. Expression of the Pax2 gene in human fetal kidney and wilms-tumor. *Cell Growth & Differentiation.* 3:279-289.
28. Quiring, R., U. Walldorf, U. Kloter and W. J. Gehring. 1994. Homology of the eyeless gene of *Drosophila* to the Small eye gene in mice and Aniridia in humans. *Science.* 265:785-9.
29. Hanson, I. M., A. Seawright, K. Hardman, S. Hodgson, D. Zaletayev, G. Fekete and V. van Heyningen. 1993. PAX6 mutations in aniridia. *Hum Mol Genet.* 2:915-20.
30. Mirzayans, F., W. G. Pearce, I. M. MacDonald and M. A. Walter. 1995. Mutation of the PAX6 gene in patients with autosomal dominant keratitis. *Am J Hum Genet.* 57:539-548.
31. Azuma, N. A. Y., Masoa. 1998. Missense Mutation at the C terminus of the PAX6 Gene in Ocular Anterior Segment Anomalies. *Investigative Ophthalmology and Visual Science.* 39:828-830.

32. Grindley, J. C., D. R. Davidson and R. E. Hill. 1995. The role of Pax-6 in eye and nasal development. *Development*. 121:1433-42.
33. Glaser, T., L. Jepeal, J. G. Edwards, R. Young, J. Favor and R. L. Maas. 1994. PAX6 gene dosage effect in a family with congenital cataracts, aniridia, anophthalmia and central nervous system defects. *Nat Genet*. 7:463-469.
34. Halder, G., P. Callaerts and W. J. Gehring. 1995. Induction of ectopic eyes by targeted expression of the eyeless gene in *Drosophila*. *Science*. 267:1788-92.
35. Mears, A. J., T. Jordan, F. Mirzayans, S. Dubois, T. Kume, M. Parlee, R. Ritch, B. Koop, W. L. Kuo, C. Collins, J. Marshall, D. B. Gould, W. Pearce, P. Carlsson, S. Enerback, J. Morissette, S. Bhattacharya, B. Hogan, V. Raymond and M. A. Walter. 1998. Mutations of the forkhead/winged helix gene, FKHL7, in patients with Axenfeld-Rieger anomaly. *Am J Hum Genet*. 63:1316-1328
36. Nishimura, D. Y., R. E. Swiderski, W. L. M. Alward, C. C. Searby, S. R. Patil, S. R. Bennet, A. B. Kanis, J. M. Gastier, E. M. Stone and V. C. Sheffield. 1998. The forkhead transcription factor gene FKHL7 is responsible for glaucoma phenotypes which map to 6p25. *Nat Genet*. 19:140-147.
37. Shields, M. B., E. Buckley, G. K. Klintworth and R. Thresher. 1985. Axenfeld-Rieger syndrome. A spectrum of developmental disorders. *Surv Ophthalmol*. 29:387-409.
38. Kunkel, L., Smith, K., Boyer, S., Borgaorkar, D., Wachtel, S., Miller, O., Breg, W., Jones, H., Rary, J. 1977. Analysis of human Y-chromosome-specific reiterated DNA in chromosome variants. *P.N.A.S.* 74:1245-1249.
39. Madisen, L., D. I. Hoar, C. D. Holroyd, M. Crisp and M. E. Hodes. 1987. DNA banking: The effect of storage of blood and isolated DNA on the integrity of DNA. *Am. J. Med. Genet*. 27:379-390.
40. Gage, P. J. and S. A. Camper. 1997. Pituitary homeobox 2, a novel member of the *bicoid*-related family of homeobox genes, is a potential regulator of anterior structure formation. *Hum Mol Genet*. 6:457-464.

41. Nichols, B. E., E. M. Stone and V. C. A. Sheffield. 1993. User-friendly Macintosh interface for DOS-based linkage analysis. *CABIOS*. 9:757-9.
42. Sheffield, V. C., E. M. Stone, W. L. M. Alward, A. V. Drack, A. T. Johnson, L. M. Streb and B. E. Nichols. 1993. Genetic-linkage of familial open-angle glaucoma to chromosome-1q21-q31. *Nat Genet*. 4:47-50.
43. Stone, E. M., A. E. Kimura, J. C. Folk, S. R. Bennett, B. E. Nichols, L. M. Streb and V. C. Sheffield. 1992. Genetic linkage of autosomal dominant neovascular inflammatory vitreoretinopathy to chromosome 11q13. *Hum Mol Genet*. 1:685-9.
44. Morton, N. E. 1955. Sequential test for the detection of linkage. *Am J Hum Genet*. 8:80-96.
45. Church, G. M. and W. Gilbert. 1984. Genomic sequencing. *P.N.A.S., USA*. 81:1991-95.
46. Chisholm, I. A. and A. E. Chudley. 1983. Autosomal dominant iridogoniodysgenesis with associated somatic anomalies: four-generation family with Rieger's syndrome. *Brit. J. Ophthal*. 67:529-534.
47. Schinzel, A. E. A. 1997. Multiple congenital anomalies including Rieger eye malformation in a boy with interstitial deletion of (4)(q25-27) secondary to a balanced insertion in his normal father: evidence for haplotype insufficiency causing the Rieger malformation. *Journal of Medical Genetics*. 34:1012-1014.
48. Flomen, V., R. Vatcheva, P. Gorman, P. Baptista, J. Groet, I. Barisic, I. Ligutic, D. Nizetic. 1998. Construction and Analysis of a Sequence-Ready Map in 4q25: Rieger Syndrome can be Caused by Haploinsufficiency of RIEG but also by Chromosome Breaks 90 kb Upstream of this Gene. *Genomics*. 47:409-413.
49. Kulharya, A. S., M. Maberry, M. K. Kukulich, D. W. Day, N. R. Schneider, G. N. Wilson and V. Tonk. 1995. Interstitial deletions 4q21.1q25 and 4q25q27: Phenotype variability and relation to Rieger anomaly. *Am J Med Genet*. 55:165-170.

50. Makita, T., M. Masuno, K. Imaizumi, S. Yamashita, S. Ohba, I. Daizou and Y. Kuroki. 1995. Rieger Syndrome with de novo reciprocal translocation t(1;4) (q23.1;q25). *Am J. Med Genet.* 57:19-21.
51. Ligutic, I., L. Brecevic, I. Petkovic, T. Kalogjera and Z. Rajic. 1981. Interstitial deletion 4q and Rieger syndrome. *Clin. Genet.* 20:323-327.
52. Semina, E.V., N. Datson, N. Leysens, B. Zabel, J. Carey, G. Bell, P. Bitoun, C. Lindgren, T. Stevenson, R. Frants, G. Ommen, J. Murray. 1996. Exclusion of Epidermal Growth Factor and High Resolution Physical Mapping across the Rieger Syndrome Locus. *Am. J. Hum. Genet.* 59:1288-1296.
53. Datson, N., E. Semina, S. Staalduinen, H. Dauwerse, E. Meershoek, J. Heus, R. Frants, J. Dunnen, J. Murray, G. Ommen. 1996. Closing in on the Rieger Syndrome Gene on 4q25: Mapping Translocation Breakpoints within a 50kb Region. *Am. J. Hum. Genet.* 59:1297-1305.
54. Burglin, T. R. 1994. Guidebook to the Homeobox Genes. Sambrook and Tooze, Oxford University Press, Geneva, Switzerland.
55. Scott, M. P., Tamkun, J. W., Hartzell, G. W. III. 1989. The Structure and Function of the Homeodomain. *Biochem. and Biophys. Acta.* 989:25-48.
56. Kissinger, C. R. 1990. Crystal structure of an engrailed homeodomain-DNA complex at 2.8Å resolution: a framework for understanding homeodomain-DNA interactions. *Cell.* 63:579-590.
57. Pearce, W. G. 1986. Corneal involvement in autosomal dominant coloboma/microphthalmos. *Canadian Journal of Ophthalmology.* 21:291-4.
58. Alward, W. L., E. V. Semina, W. Kalenak, E. Heon, B. P. Sheth, E. M. Stone and J. C. Murray. 1998. Autosomal dominant iris hypoplasia is caused by a mutation in the Rieger Syndrome (RIEG/PITX2) gene. *Am J Ophthalmol.* 125:98-100.

59. Hanson, I. M., J. M. Fletcher, T. Jordan, A. Brown, D. Taylor, R. J. Adams, H. H. Punnett and V. van Heyningen. 1994. Mutations at the PAX6 locus are found in heterogeneous anterior segment malformations including Peters anomaly. *Nat Genet.* 6:168-173.
60. Semina E., R. Ferrel, H. Mintx-Hittner, P. Bitoun, W. Alward, R. Reiter, C. Funkhauser, S. Daack-Hirsch, J. Murray. 1998. A novel homeobox gene PITX3 is mutated in families with autosomal-dominant cataracts and ASMD. *Nat Genet.* 19:167-170.
61. Meno, C. E. A. 1996. Left-Right asymmetric expression of the TGFB-family member *lefty* in mouse embryos. *Nature.* 381:151-158.
62. Meno, C. E. A. 1998. *lefty-1* is Required for Left-Right Determination as a Regulator of *lefty-2* and *nodal*. *Cell.* 94:287-297.
63. Issac, A., Sargent, M., Cooke, J. 1997. Control of vertebrate Left-Right Asymmetry by a *Snail*-Related Zinc Finger Gene. *Science.* 275:1301-1304.
64. Levin, M., Johnson, R., Stern, C., Kuehn, M., Tabin, C. 1995. A Molecular Pathway Determining Left-Right Asymmetry in Chick Embryogenesis. *Cell.* 82:803-814.
65. Harvey, R. 1998. Links in the Left/Right Axial Pathway. *Cell.* 1998:273-376.
66. Logan, M., Pagan-Westphal, S., Smith, D., Paganessi, L., Tabin, C. 1998. The Transcription Factor Pitx2 Mediates Situs-Specific Morphogenesis in Response to Left-Right Asymmetric Signals. *Cell.* 94:307-317.
67. Hyatt, B. A. Y., Joseph. 1998. The Left-Right Coordinator: The Role of *Vgl* in Organizing the Left-Right Axis Formation. *Cell.* 93:37-46.
68. Pagan-Westphal, S. A. T., Clifford. 1998. The transfer of Left-Right Positional Information during Chick Embryogenesis. *Cell.* 93:25-35.
69. Piedra, M. E., J. M. Icardo, M. Albajar, J. C. Rodriguez-Rey and M. A. Ros. 1998. Pitx2 participates in the late phase of the pathway controlling left-right asymmetry. *Cell.* 94:319-324.

70. Yoshioka, H., C. Meno, K. Koshiba, M. Sugihara, H. Itoh, Y. Ishimaru, T. Inoue, H. Ohuchi, E. V. Semina, J. C. Murray, H. Hamada and S. Noji. 1998. Pitx2, a bicoid-type homeobox gene, is involved in a lefty-signalling pathway in determination of left-right asymmetry. *Cell*. 94:299-305.
71. Amend, S., L. Sutherland, E. Semina, A. Russo. 1998. The Molecular Basis of Rieger Syndrome. *J. of Biological Chemistry*. 273:20066-20072.
72. Simmons, D. E. A. 1990. Pituitary cell phenotypes involve cell-specific Pit-1 mRNA translation and synergistic interactions with other classes of transcription factors. *Genes and Development*. 4:695-711.
73. Holloway, J. M., D. P. Szeto, K. M. Scully, C. K. Glass and M. G. Rosenfeld. 1995. Pit-1 binding to specific DNA sites as a monomer or dimer determines gene-specific use of a tyrosine-dependent synergy domain. *Genes & Development*. 9:1992-2006.
74. Mangalam, H. E. A. 1989. A pituitary POU domain protein, Pit-1, activates both growth hormone and prolactin promoters transcriptionally. *Genes and Development*. 3:946-958.
75. Flomen, R., Gorman, P., Vatcheva, R., Groet, J., Barisic, I., Ligutic, I., Shoer, D., Nizetic, D. 1997. Rieger Syndrome Locus: a new reciprocal translocation t(4;12)(q25;q15) and a deletion (4)(q25q27) both break between markers D4S2945 and D4S193. *Journal of Medical Genetics*. 34:191-195.
76. Shields, M. B. 1983. Axenfeld-Rieger syndrome: a theory of mechanism and distinctions from the iridocorneal endothelial syndrome. *Trans Am Ophthalmol Soc*. 81:736-84.
77. Mirzayans et. al., in press